Cell Reports Physical Science

Review

Mechanical energy-induced charge separation in intelligent sensing

Wenjie Wang,[1,3] Hua Xiao,[1,3] Lei Zhang,[1,3] Yingfei Wang,[1] Quan Yuan,[1,2,*] and Jie Tan[1,*]

SUMMARY

Mechanical sensors play a pivotal role in intelligent sensing and exhibit exciting prospects for applications including human-machine interactions and biomedical engineering. However, the applicability of mechanical sensors has been greatly restricted, owing to the reliance on external power supplies. Interfacial charged materials can harvest mechanical energy to induce charge separation and output electricity, therefore eliminating the bottleneck of the power source. Previous researchers have reviewed the widespread applications of interfacial charged materials, whereas the energy conversion mechanisms of interfacial charged materials and their applications in intelligent sensing are not well discussed. Here, the energy conversion, development, and applications of interfacial charged materials in intelligent sensing are systematically reviewed.

INTRODUCTION

Intelligent sensing has taken off at a brisk speed in industry and life.[1] Mechanical sensors are crucial components of intelligent sensing, and are becoming interdisciplinary hotspots in electronics, materials science, chemistry, computer science, and so on.[2–6] In intelligent sensing systems, mechanical sensors convert mechanical energy to electrical signal, and they further interact with other terminal devices to perceive the environment and our bodies.[3,5,7] However, the strong demand for power supply has prevented mechanical sensors from working continuously, especially working as implantable devices in the body.[8–10] For instance, intelligent pacemakers can provide pre-warning of heart disease based on heart rate, yet the continuous work of pacemakers remains challenging because the lifetime of power sources is limited.[11,12] Hence, overcoming power shortage and improving practicability of mechanical sensors are pressing issues in the field of intelligent sensing.[6,10]

Interfacial charging of material serves as a potential strategy for power supply.[10,13–16] Mechanical energy-induced charge separation can be exploited as a continuous power source of intelligent devices.[10] Meanwhile, variation of output electric signal reflects the change in mechanical energy applied on materials.[13] When a material is subjected to mechanical energy, charge separation occurs at the interface by internal polarization or charge transfer.[15–18] As the mechanical energy applied on material changes, the charge distribution at the interface also varies.[5,13] That interfacial charging eventually generates an electric field varying with mechanical energy. Then electrons are further output to external circuit via electrostatic induction.[19,20] For that reason, it is important to synthesize interfacial charged materials for mechanical energy harvesting, and explore the connection between their electrical properties and physical/chemical structures, so as to develop mechanical-responsive intelligent sensors.[4,6,20]

[1]Molecular Science and Biomedicine Laboratory (MBL), Institute of Chemical Biology and Nanomedicine, State Key Laboratory of Chemo/Biosensing and Chemometrics, College of Chemistry and Chemical Engineering, Hunan University, Changsha 410082, China

[2]College of Chemistry and Molecular Sciences, Wuhan University, Wuhan 430072, China

[3]These authors contributed equally

*Correspondence: yuanquan@whu.edu.cn (Q.Y.), tanjie0416@hnu.edu.cn (J.T.)

CellPress
OPEN ACCESS

Cell Reports
Physical Science
Review
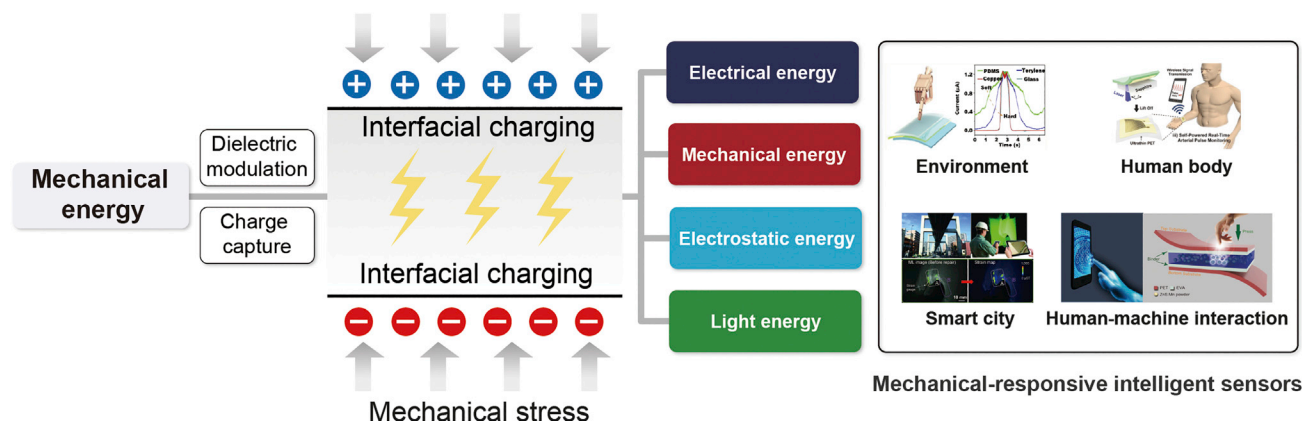
Figure 1. Schematic illustration of mechanical-responsive intelligent sensors enabled by interfacial charging
Reproduced with permission from Park et al.[24] Copyright 2017, Wiley-VCH. Reproduced with permission from Li et al.[25] Copyright 2017, American Chemical Society. Reproduced with permission from Liu et al.[26] Copyright 2019, Wiley-VCH. Reproduced with permission from Tang et al.[27] Copyright 2020, Wiley-VCH. Reproduced with permission from Wang et al.[28] Copyright 2015, Wiley-VCH.

Interfacial charging is important to mechanical-responsive intelligent sensors, and effectively implements mechanical-to-electrical energy conversion in intelligent devices. Interfacial charging can convert mechanical energy widely present in the environment into electrical energy to overcome power shortage of intelligent devices. On the other hand, the energy conversion in interfacial charging can derive light energy, mechanical energy, and other kinds of energy. These conversions can greatly enrich interaction mode and provide all-sided energy supply, which is of great value to intelligent interaction. Previous reviews have demonstrated the widespread applications of interfacial charged materials.[10,21–23] In order to enhance interfacial charging, researchers have made great efforts in crystal growth, chemical modification, surface engineering, and so on.[3,5] However, the energy conversion by interfacial charging and its exploitation in intelligent sensing are still not well reviewed. To elaborate on the significance of mechanical-responsive interfacial charging, this review discusses the development and applications of mechanical-responsive intelligent sensors from the perspective of interfacial charged materials. The content includes (1) the mechanism of interfacial charging and energy conversion, (2) the design of interfacial charged materials, and (3) the mechanical energy responded to by interfacial charged materials (Figure 1).

THE PRINCIPLES OF MECHANICAL ENERGY INDUCING INTERFACIAL CHARGE

Thus far, the principles of mechanical energy-induced interfacial charging usually include internal polarization of material and contact between two dissimilar material interfaces. These two processes both lead to the generation of time-varying electric fields at material interfaces. These electric fields are suggested to further generate displacement current, which is responsible for electricity transport in capacitive conduction.[20] Apart from these principles, fracture of crystal can also lead to interfacial charging sometimes, whereas that process is usually not reproduceable.[29] Therefore, elastic deformation rather than fracture of crystal is included in this review.

Interfacial charging by internal polarization

Among the dielectrics, there is a class of materials that their dipole moment can change under the action of external pressure. That phenomenon leads to internal polarization of the material, making the upper and lower interfaces charged (Figure 2A). Those materials are named piezoelectric materials. Piezoelectric materials are usually crystals with

non-centrosymmetric structure. By applying external pressure in an oriented direction, the piezoelectric material is mechanically deformed. In this way, the offset of positive and negative centers inside the unit cell is destroyed in the direction of pressure. The dipole moment inside the material is therefore changed, such as ZnO_4 tetrahedra in wurtzite-structured ZnO (Figure 2B).[16] The charges are retained until the pressure disappears, making upper and lower interfaces charged. When pressure is applied again, the polarization reappears. The accumulated charges at interfaces transfer to electrodes and external circuit by electrostatic induction. Besides non-centrosymmetric crystals, piezoelectricity has also been found to be present in regions near chemical or physical defects in centrosymmetric crystals.[30–32] Crystals in nature are always defective, and local lattice distortions can cause weak piezoelectricity in defective regions of centrosymmetric crystals.[31] In addition, researchers have recently discovered that the interfacial properties of some centrosymmetric crystals, such as Schottky junctions formed by noble metals and centrosymmetric semiconductors, enable these crystals to exhibit piezoelectric effects.[33]

Another class of piezoelectric materials with unique properties, ferroelectric materials, are often polycrystals composed of domains with spontaneous polarization at certain temperatures. The intensity and orientation of polarization can change with mechanical deformation, so ferroelectric materials exhibit strong piezoelectric effect.[16] This self-polarization results from a slight distortion of crystal structure, so that their positive and negative centers separate.[36] For example, in oxygen octahedra of perovskite-structured compounds, central metal cations deviate from the geometric center of the octahedra, leading to distortion and polarization (Figure 2C). It is worth noting that when the temperature exceeds a certain value, namely Curie temperature, vibration of atoms in lattice is strong enough to break the spontaneous polarization of ferroelectric materials. This special state is named the paraelectric phase.[37] In the paraelectric phase, the interfacial charging properties of ferroelectric materials change greatly, and the piezoelectricity is usually very weak. Therefore, the supposed temperature range of applications needs to be taken into consideration in the design of ferroelectric materials. In spite of the slight distortion and polarization, when the overall voltage is applied to ferroelectric materials, their polarization switches in line with the direction of electric field (Figure 2D).[38] In this way, ferroelectric materials can also produce ordered interfacial charging as the common result of spontaneous internal polarization and mechanical energy-induced internal polarization. In addition, their piezoelectric coefficient, a factor that reflects how applied stress induces polarization, is usually much higher than piezoelectric single crystal. That means ferroelectric materials can provide stronger interfacial charging.

Interfacial charging by contact electrification

In contrast to internal polarization by applied stress, interfacial charging by contact between materials is quite different. That is essentially the charge transfer between two interfaces, namely contact electrification (Figure 2E). The driving force of contact electrification, also known as triboelectrification, is still an outstanding issue. A widely accepted explanation is that the electron affinity energy of atoms at different interfaces is disparate. On the other hand, ion transfer is also believed to exist in contact electrification in some cases (Figure 2F).[15]

The well-accepted explanation of electron transfer is described as follows. When intimate contact occurs, the atoms at interfaces are so close to each other that the electron orbitals partially overlap (Figure 2G), during which covalent bonds are supposed to be formed.[15,35] Because of the difference in electron affinity energy, electrons escape from the atoms that tend to lose electrons, while atoms with strong electron affinity gain the electrons. When the interfaces are separated, electrons
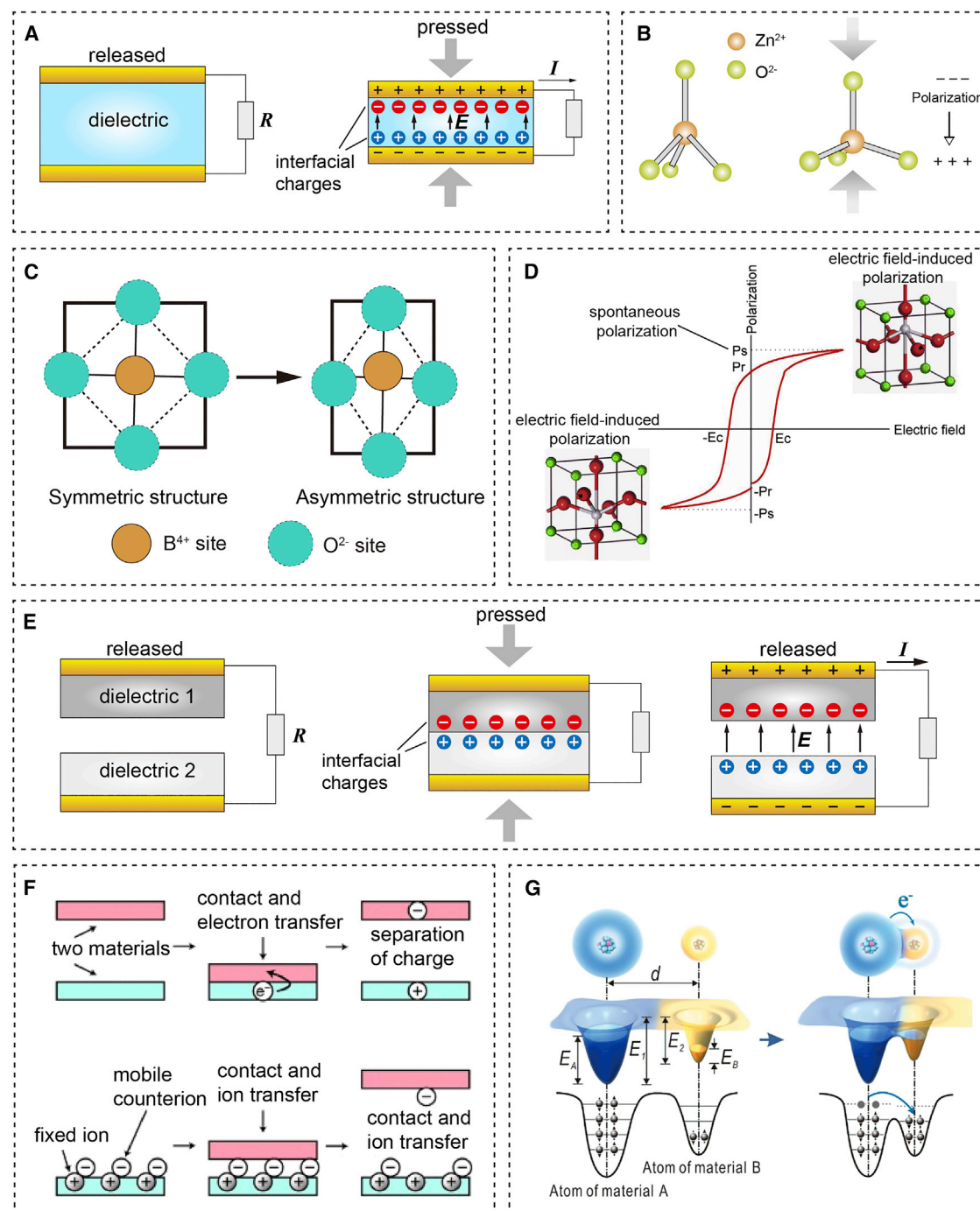
Figure 2. The principles of mechanical energy inducing charge separation and interfacial charging

(A) Schematic illustration of internal polarization inducing interfacial charge under pressure.

(B) Dipole moment change of piezoelectric crystal ZnO under pressure.

(C) Illustration of perovskite ferroelectric material that is undergoing spontaneous polarization due to lattice distortion of octahedra.

(D) The ferroelectric hysteresis loop that reflects how applied electric field influences the polarization of ferroelectric material. Reproduced with permission from Gao et al.[34] Copyright 2020, Elsevier.

(E) Illustration of interfacial charging due to contact electrification.

(F) Schematic diagram of electron (top) or ion (bottom) transfer mechanism of contact electrification. Reproduced with permission from McCarty et al.[15] Copyright 2008, Wiley-VCH.

(G) Schematic diagram of electron transfer resulting from partial overlap of atomic orbitals at interface. Reproduced with permission from Xu et al.[35] Copyright 2018, Wiley-VCH.

CellPress
OPEN ACCESS

trapped at the interface are retained because a barrier prevents tunneling, making one interface negatively charged and another one positively charged. With repeated contact and separation, the distance between the interface changes, thus generating electrostatic induction and current output. Although metal is not dielectric, it can also be involved in contact electrification by using work function to explain the tendency of electron transfer.[39] Effects of the Schottky barrier may also need to be considered when metal contacts with semiconductors, because Schottky barrier can prevent contact electrification in some instances.[40] In addition to the contact between solid and solid, solid and liquid or gas can also induce contact electrification.[41] Ion transfer is also involved in contact electrification sometimes. The ion transfer mechanism can explain why some organic materials exhibit a distinct ability to acquire charges during contact.

Ion transfer is responsible for many electrodynamic phenomena, such as electroosmosis, electrophoresis, and streaming potential. However, some microscopic and macroscopic experiments have shown that electrons also participate in contact electrification of the solid-liquid interface and play an important role in the formation of the electric double layer. Solid-liquid interface is an important interface in physical and chemical reactions. Because of motion of ions and electrons at solid-liquid interface, ion transfer and electron transfer are both involved in contact electrification and formation of electric double layer. The contact electrification mechanism at the solid-liquid interface is considered to have two steps: electron exchange and ion adsorption.[42] Electron transfer at a virgin surface may be the first step of contact electrification at a solid-liquid interface. The subsequent electrostatic interaction and ion adsorption further lead to the formation of intact electric double layer.[43,44]

In contact electrification, the mechanical stress does not cause mechanical deformation like that in piezoelectric materials. The mechanical energy makes the interfaces of two materials contact and separate. The contact only generates electrostatic charges at interfaces. Only when displacement occurs between two interfaces can the interfacial charges be transformed into electrical energy via electrostatic induction. Therefore, the mode of relative movement between interfaces also affects output.[10] The most common mode is the vertical contact-separation mode, which is similar to internal polarization of piezoelectric materials. Another frequently used mode is that one interface moves laterally along another interface.[20] Recently, motion forms of interfacial charged materials for contact electrification have been greatly enriched, including rolling mode, peeling mode, and free-standing powder mode.[45,46,47] Also, many sophisticated mechanical structures have been developed to promote relative movement of different materials.[48] These novel forms of motion can help efficiently harvest various mechanical energies and achieve continuous work, thus improving the electrical output of interfacial charged materials.

INTERFACIAL CHARGING INDUCES GENERATION OF OTHER ENERGY

After interfacial charged materials generate interfacial charges, the charges can be transferred to the capacitor, and the electricity can be stored for power supply or signal acquisition. On the other hand, the generated electrical energy can also induce other energy (e.g., light energy). This capacity greatly widens the applicability of interfacial charged materials in intelligent devices.

Interfacial charging generates mechanical energy

Two charged interfaces of materials can produce a very large potential difference. In contact electrification, plentiful electrostatic charges accumulated at interfaces can
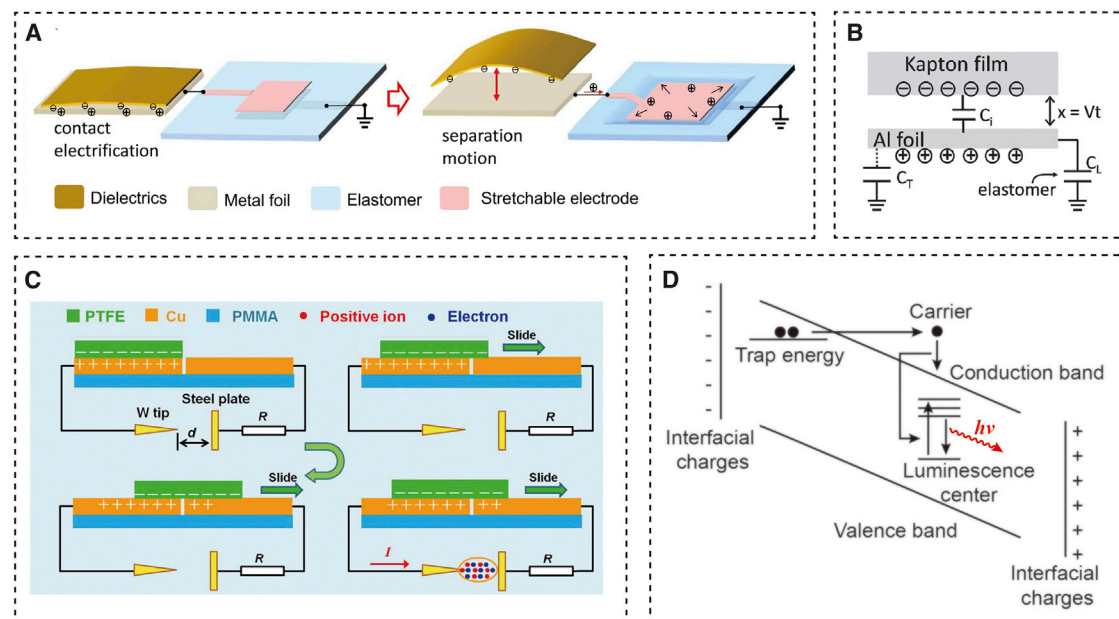
Figure 3. Mechanisms of interfacial charging inducing generation of other energy
(A) Schematic diagram of actuated strain of dielectric elastomer caused by interfacial charging. Reproduced with permission from Chen et al.[59] Copyright 2017, Elsevier.
(B) Circuit diagram of connection between interfacial charged materials and dielectric elastomer. Reproduced with permission from Chen et al.[54] Copyright 2016, Wiley-VCH.
(C) Schematic diagram of an air discharge driven by interfacial charging-elicited high voltage. Reproduced with permission from Cheng et al.[60] Copyright 2018, Elsevier.
(D) Mechanism of trap-based interfacial charging generating light energy.

give rise to open-circuit voltage output of even more than 1,000 V.[49,50] This huge open-circuit voltage is able to drive mechanical deformation of dielectric elastomers, so as to further convert the electrical energy generated by interfacial charged materials into mechanical energy for human-machine interaction.[51] Likewise, internally polarized interfacial charged materials can also be used to drive the dielectric elastomer actuation.[52,53] Dielectric elastomer is a material that can produce large mechanical deformation under applied electric field across thickness direction. After the charges generated by interfacial charged materials are transferred to the parallel-plate capacitor, the dielectric elastomer located between plates or electrodes will be squeezed in the vertical direction (Figures 3A and 3B), while the Maxwell stress of dielectric elastomer is related to electric field.[54,55,56] In addition, interfacial charging can also be converted into mechanical energy by driving the movement of metal via electrostatic induction, or utilizing electric force to drive the movement of charged object. For example, interfacial charging can drive electrospinning. High-voltage electric field generated by contact electrification can charge polymer solution or melt, and further help solution or melt overcome surface force in the tube.[57] In this way, fluid jet can produce polymer nanofibers. That high voltage can also be employed to realize oil-water separation. The alternating electric field generated by contact electrification will make originally charged water droplets in oil reciprocate. This electric field accelerates the collision and aggregation of water droplets so as to achieve oil-water separation.[58]

Interfacial charging generates electrostatic energy
Interfacial charged materials have high voltage output. When two interfaces are charged, a huge electrostatic field can be generated between two interfaces of

CellPress
OPEN ACCESS

interfacial charged materials or two plates of a capacitor, thus generating large electrostatic energy. Electrostatic field can change the direction or velocity of moving charges, as well as charged droplets and particles.[61,62] Compared with the traditional high-voltage electric field generation equipment, this strategy is obviously safer, simpler, and low cost, and has good application prospects in electrostatic dust collection, microfluidic technology, droplet separation, and other fields. In addition, the interfacial charged materials can also be employed to realize air discharge when it generates a high voltage up to the breakdown voltage between capacitors. This property can be used to construct an air discharge switch (Figure 3C).[60]

Interfacial charging generates light energy

Mechanoluminescence is a physical phenomenon of mechanical-light energy conversion in interfacial charged materials. Trap plays an important role in mechanoluminescence.[63,64] Thus, a well-accepted explanation of mechanoluminescence in interfacial charged materials is similar to the mechanism of persistent luminescence.[65] Interfacial charged materials provide huge voltage for excitation of charge carrier in trap, while the excitation of persistent luminescence materials originates from thermal disturbance.[64,66,67] When interfacial charged material is under external stress, charge distribution at interfaces and high voltage are induced. The high voltage between interfaces makes the conduction band and valence band of material tilt. Then electrons in trap will be excited to conduction band, followed by transition across energy level and recombination of electrons and holes. All these processes finally give rise to excitation and luminescence of the luminescence center (Figure 3D).[68,69] For example, ZnS doped with Mn is polarized under pressure, and the inner electric field induced by interfacial charges excites the carriers in trap and finally produces orange luminescence of Mn.[28,29] Contact electrification can also give rise to triboluminescence of some materials. The contact and separation at material interfaces can discharge. Then electric field induced at interfaces often leads to recombination of carriers and electron transition within materials. Therefore, in many cases, triboluminescence of interfacial charged materials is caused by contact electrification-induced electroluminescence.[70–72] The triboluminescence intensity during contact electrification is closely related to the type of contact material. Moreover, cleavage, peeling, grinding, crushing, and many other processes can also lead to discharge at interface, thus converting mechanical energy into light energy.[73–75] These forms of mechanoluminescence have long been discovered, but their mechanisms are still not fully understood, such as the possible breaking of chemical bonds and the subsequent process that charges surrounding interfaces.[64]

Mechanoluminescence imparts new function and application scenarios to interfacial charged materials. Interfacial charged materials are frequently used to construct mechanoluminescence-based sensors, because generation of electric field by interfacial charged materials is usually non-destructive and repeatable. Rather, charged dislocation-induced mechanoluminescence, another mechanism that originates from the fracture of crystal, is usually unrepeatable and seldom utilized.[29]

THE DESIGN OF INTERFACIAL CHARGED MATERIALS

After understanding the response principle of interfacial charged materials, how to promote energy conversion efficiency is of great significance. Here, we discuss how to select suitable interfacial charged materials and elevate their interfacial charges to produce high output.
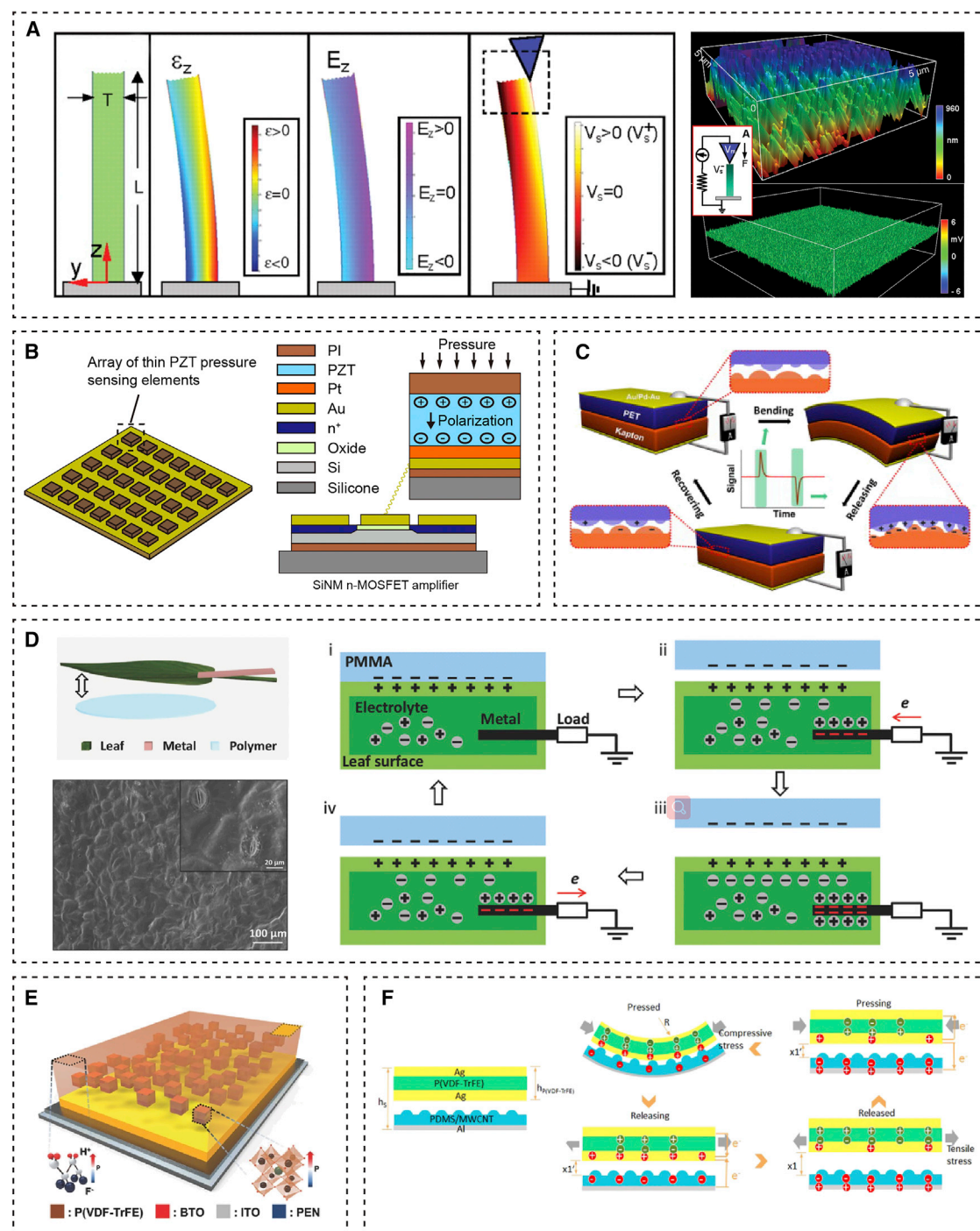
Figure 4. Several interfacial charged materials and their response mechanisms

(A) The structure and output distribution of ZnO nanowires. Reproduced with permission from Wang et al.[77] Copyright 2006, The American Association for the Advancement of Science.

(B) Schematic diagram of fabrication of PZT nanoarrays and internal polarization under pressure.[78]

(C) Working mechanism of PET film and Kapton film producing contact electrification. Reproduced with permission from Fan et al.[79] Copyright 2012, Elsevier.

(D) Structure and working principle of leaf and PMMA as interfacial charged materials for contact electrification. Reproduced with permission from Jie et al.[80] Copyright 2018, Wiley-VCH.

**Cell Reports
Physical Science**
Review

CellPress
OPEN ACCESS

Interfacial charged materials with internal polarization

Piezoelectric effect is the ability of material to transform mechanical deformation into interfacial charging. Piezoelectric material usually features non-centrosymmetric structure. In this regard, we can predict which crystals may have piezoelectric effects.[76] Of the 32 crystal point groups, only 20 of them are likely to have piezoelectric effects due to non-centrosymmetric structure, except point group 432 with high symmetry.[16] Among these materials, there are many commercialized piezoelectric materials, including wurtzite (ZnO) and quartz (SiO_2). In piezoelectric single crystal, the direction of polarization inside the material is determined by the orientation of the crystal. These non-centrosymmetric materials are often synthesized as bulk crystals, or oriented polycrystalline samples (such as arrays or films). Wang et al.[77] first constructed aligned ZnO nanowire arrays to scavenge mechanical energy (Figure 4A). Vast ZnO nanowires are oriented on the bottom electrode. The ZnO nanowire is bent under the pressure of Pt tip, and the positive and negative charges are produced at ZnO interface. The contact between Pt tip and ZnO at a specific location results in rapid electron transfer and current output between interfaces. Although plentiful crystals found in nature are centrosymmetric and do not have piezoelectric effects, researchers have found that piezoelectricity can be induced in centrosymmetric structures. Yang et al.[33] showed that built-in electric field induced interfacial polar symmetry, resulting in apparent piezoelectric properties in centrosymmetric material.

Ferroelectric materials possess spontaneous polarization at certain temperatures and the polarization can be reversed under electric field. High-voltage polarization is usually necessary to prepare ferroelectric materials.[83] Ferroelectricity often involves octahedral coordination d_0 transition metal cations, as well as cations with lone electron pairs, such as perovskite compounds (ABO_3).[16] In perovskite materials, a series of ferroelectric materials with different crystal structures and properties can be obtained by changing the types of metal cations. For example, $BaTiO_3$, $PbTiO_3$, and $Pb(Zr_x,Ti_{1-x})O_3$ (PZT) can be divided into A and B site doping according to the doping site of metal ions.[84] Lone electron pairs also enhance interfacial charging by introducing distortion. Ferroelectric materials usually exhibit stronger interfacial charging in comparison with piezoelectric single crystals. In addition, the preparation of ferroelectric materials often does not require bulk crystal growth, and is therefore suitable for fabricating arrays and thin films. Dagdeviren et al.[78] designed a pressure sensor using square PZT arrays that are integrally connected to adjacent gate electrodes (Figure 4B). Such arrays coupled with flexible substrates are expected to overcome the rigidity problem of inorganic materials. However, ferroelectric materials with strong interfacial charging usually contain toxic heavy metal ions, which make them poor candidates for biomedical applications at present.[85] That is an important challenge for ferroelectric materials. Given this, ferroelectric polymers have been well developed in the past because ferroelectric polymers are considered to be biocompatible and flexible, which may be beneficial to biomedical applications. However, polymer-based flexible ferroelectric materials usually exhibit weak piezoelectricity. Recently, molecular design of ferroelectric materials has been proposed to overcome the toxicity and rigidity of traditional ferroelectric materials.[83,85] In this way, the discovery and design of ferroelectric materials can be oriented toward chemical design and synthesis. Molecular ferroelectric materials are not only flexible and biocompatible but also show prominent piezoelectricity and interfacial charging.

(E) Structure of hybrid interfacial charged materials fabricated by internally polarized P(VDF-TrFE) and inner dielectric ceramic $BaTiO_3$ (BTO). Reproduced with permission from Seung et al.[81] Copyright 2017, Wiley-VCH.

(F) Working principle of hybrid interfacial charged materials composed of P(VDF-TrFE) with internal polarization and PDMS/MWCNT for contact electrification. Reproduced with permission from Wang et al.[82] Copyright 2016, Springer Nature.

Table 1. The empirical ranking of interfacial charging ability of several materials during contact electrification

Tendency to acquire charge	Interfacial charged materials for contact electrification
Most positively charged in this table	glass
	polyamide (nylon 6,6)
	NaCl
	silica
	silk
	aluminum
	amber
	copper
	silver
	gold
	polystyrene
	polyethylene
Most negatively charged in this table	PTFE

Interfacial charged materials with contact electrification

Apart from internal polarization, materials with contact electrification can also generate interfacial charges under mechanical stress. When contacting at an interface (the interface can be solid, liquid, or even gas), contact electrification has unconsciously taken place. The first report of contact electrification can be traced back to ancient Greece, where amber and fur produced charge separation when they were rubbed together.[15] As mentioned above, contact electrification exists on the premise that the difference in electron affinity energy of two interfaces is large, allowing electrons to transfer from one interface to the other.[86,87] An empirical ranking table of interfacial charging ability (Table 1) has been listed based on the experimental results of interfacial charging.[15] At the lower part of the table, materials are apt to gain more negative charges in contact due to strong electron-capturing ability. At the upper part of the table, positive charge generation is preferred. It is noted that non-polar materials like polytetrafluoroethylene (PTFE) have a tendency to produce strong negative interfacial charges during contact. Some researchers suggested that the process involves electron transfer between interfacial functional groups, and others proposed that it involves ion transfer processes.[15]

Compared with internally polarized materials, the interfacial charged materials for contact electrification are usually non-toxic and ubiquitous in nature. Since organic polymers exhibit strong electron-capturing ability and large dielectric constant, the charges are readily retained at interfaces. Moreover, organic polymers have good flexibility, so they are ideal candidates for interfacial charged materials. Fan et al.[79] employed Kapton film and polyethylene terephthalate (PET) film as interfacial charged materials. They are sandwiched by top and bottom gold electrodes (Figure 4C). Under bending conditions, Kapton interface and PET interface generated negative and positive charges respectively. Finally, voltage output of 3.3 V could be achieved during contact and separation. Using metal electrodes as the interfacial charged materials for contact electrification is another strategy because metal electrodes tend to lose electrons. Yang et al.[88] developed interfaces consisting of Al film and PTFE film with Al positively charged and PTFE negatively charged upon contact. Recently, semiconductor nanomaterials are emerging as prominent interfacial charged materials for contact electrification. They are used to regulate the charge transfer at interfaces due to their electrical properties. For example, metal and perovskite nanomaterials are chosen as a pair of interfacial charged

materials for contact electrification, during which the output of metal-perovskite nanomaterials can be tuned by light. This is ascribed to the semiconductor property of perovskite nanomaterial.[89] Recently, topological semiconductor nanomaterial (Bi_2Te_3 nanoplates) was first employed as interfacial charged material because of its strong positive charging.[17] In the future, inorganic or organic semiconductors may play important roles in interfacial charging for contact electrification.

The contact electrification mechanism of inorganic materials is similar to that of polymer materials to some extent. In essence, their charge transfers are both caused by difference in the ability of atoms to capture charge after intimate contact at two interfaces.[35,90] However, the physical properties of inorganic materials and polymers are quite different, which leads to the difference of specific mechanism involved in contact electrification. Inorganic materials usually have lower resistivity and good dielectric properties. In contact electrification of inorganic materials, electron transfer is dominant. Therefore, the energy band structure has an important influence on contact electrification of inorganic materials. The work function or Fermi level will affect the direction and quantity of electron transfer.[90] Polymer materials usually have no definite Fermi level. In this case, electron-cloud-potential-well model can account for contact electrification of polymers.[91] In addition, ion transfer is thought to be involved in contact electrification of many organic polymers because there are chemical groups at interfaces that can effectively bind ions.[15] Covalent bonds underlie the chemical composition of polymers, so poor conductivity is usually observed in polymers, whereas polymer materials can be chemically modified to introduce new polar groups, thereby utilizing these polar groups to increase dielectric constant of polymer materials. In this way, charge retention and interfacial charging of polymer materials can be enhanced.[92,93]

In addition to artificial materials, researchers are finding solutions in nature. For example, human skins with high impedance are good interfacial charged materials for contact electrification.[94,95] Thus, our skin is easily charged due to the friction with clothing in dry air. Based on the interfacial charging property of skin, Yang et al.[96] designed a pair of interfacial charged materials from skin and polydimethylsiloxane (PDMS). During contact electrification, the negative charges at the PDMS interface are transferred through indium tin oxide (ITO) conductive glass. The strategy of using the human body as interfacial charged materials provides a new inspiration for designing wearable sensors. Skin-based interfacial charging can greatly simplify the structure of devices. Some natural materials, such as leaves, flower petals, and wood, have also been exploited to construct interfacial charged materials by virtue of their excellent interfacial charging properties.[97] Jie et al.[80] used natural leaves and poly(methyl methacrylate) (PMMA) to fabricate interfacial charged materials (Figure 4D). The leaves are positively charged in contact with PMMA. The rough surface structure and large contact area of the blade, as well as the electrolyte inside the blade that can conduct electricity, can effectively generate interfacial charges that result in even 45 mW m^{-2} output. Using natural materials as interfacial charged materials can make the device more eco-friendly and more biocompatible.

Hybrid interfacial charged materials

Hybrid interfacial charged materials combine the best of both internal polarization and contact electrification. This strategy includes two cases, one is to directly superimpose internally polarized material with material for contact electrification. The other is that a material can be both internally polarized and charged by contact electrification, eventually being able to use its own polarization to enhance interfacial

charging during contact. However, it should be noted that the direction of the internal polarization needs to be aligned with the electric field induced by contact electrification to realize synergistic output. Guo et al.[98] employed silk fibroin and ferroelectric poly(vinylidene fluoride) (PVDF) to fabricate interfacial charged materials. When the polarization of PVDF is in accordance with electric field created by contact between PVDF and silk fibroin, the output voltage can reach more than 70 V. When two directions are not same, the output voltage drops to 40 V in a reversed direction. To better enhance the coupling effect of internal polarization and contact electrification, Han et al.[99] conducted a theoretical study on the coupling effect of internal polarization and contact electrification. They assembled multilayers of ferroelectric PVDF with PTFE for contact electrification plus Al electrodes. They studied and compared the output performance of interfacial charged materials with different structures. They found that the voltage output of hybrid interfacial charged materials can be tuned by several factors, such as polarization directions, electrode connection modes, and coupling modes. Their study provides a theoretical basis for increasing the voltage output by coupling internal polarization and contact electrification.

The incorporation of dielectrics into interfacial charged materials is instrumental in the performance of hybrid interfacial charged materials since dielectrics with high dielectric constant can promote polarization and charge retention. Seung et al.[81] dispersed dielectric ceramic $BaTiO_3$ into ferroelectric polymer poly(vinylidenefluoride-co-trifluoroethylene), denoted as P(VDF-TrFE), to prepare nanocomposite. This nanocomposite displays strong ability of charge capture, which produces more interfacial charges during contact with Al (Figure 4E). The contact and separation of ferroelectric composites with Al can generate 1,130 V output. Semiconductors and carbon materials are also good candidates to regulate the dielectric property of hybrid interfacial charged materials. Wang et al.[82] prepared hybrid interfacial charged materials PDMS and multi-walled carbon nanotubes (MWCNT) using an electrospinning process. They dispersed MWCNT in PDMS to elevate the output voltage when PDMS/MWCNT composite film is in contact with Ag and internally polarized P(VDF-TrFE) (Figure 4F). Compared with pristine PDMS film, the as-prepared PDMS/MWCNT composite exhibits higher dielectric constant and output.

## THE STRATEGIES TO ENHANCE INTERFACIAL CHARGING

Strengthening the interfacial charging is the key to improving mechanical-electrical energy conversion efficiency, including increasing interfacial charge density, reducing impedance, and optimizing the power extraction.[100] Among them, increasing interfacial charge density has been extensively studied. That requires changes in synthesis method, crystal structure, interfacial properties, and so on. Two strategies for increasing interfacial charge density are described below.

Modulation of dielectric properties and polarizability of interfacial charged materials

Whether materials are internally polarized or charged by contact electrification, the dielectric properties are of great importance. For materials with internal polarization, it can elevate interfacial charge density by increasing the polarizability and changing dielectric constant. For materials with contact electrification, the charge storage at the interface determines the output performance, which is usually closely related to the dielectric constant of interfacial charged materials such as organic polymers.[101] Therefore, tuning the dielectric properties and polarizability of interfacial charged materials are important to enhance interfacial charging.

Changing the chemical composition of interfacial charged materials can effectively enhance the polarizability and dielectric properties. Chemical doping is an important means to strengthen polarization. For example, the internal polarization of ZnO under stress is improved after doping with Ga or Al.[102] The doped metal ions will affect the dielectric constant, energy band, carrier concentration, and rotation of bonds under stress. By changing the chemical composition and crystal structure of ferroelectric materials, the dielectric properties and piezoelectric properties can be well controlled. By doping metal cations in perovskite compounds, the polarizability and interfacial charging can be tuned. For example, doping perovskite ferroelectrics with metal cation of similar ionic radius and equivalence will cause certain lattice distortion, which may enhance the piezoelectricity. Dopants of inequivalence may hinder the domain wall motion in ferroelectric materials and weaken its interfacial charging.[103,104] In some cases, when the concentration of dopants is in an appropriate range, there will be transition in ferroelectric materials, such as tetragonal phase and tripartite phase coexistence. That transition is known as the morphotropic phase boundary (MPB). In the vicinity of the MPB, ferroelectric materials become structurally unstable and thus have strong dielectric, piezoelectric, and ferroelectric properties.[105,106] Interfacial charged materials with contact electrification are generally organic polymers. The inherent large impedance of polymers limits the current output, so semiconductors have been proposed in recent years to prepare interfacial charged materials for contact electrification. Inorganic and semiconductor materials can be chemically doped to regulate their dielectric properties and interfacial charging. Wang et al.[107] investigated the effect of alkaline earth metal doping (Mg^{2+}, Ca^{2+}, Sr^{2+}, Ba^{2+}) on the contact electrification property of $CsPbBr_3$ perovskite in contact with PVDF (Figure 5A). They found that the output of $CsPbBr_3$ decreased with increasing atomic number of doping ions except for Ba^{2+}, and the output of Ba^{2+}-doped $CsPbBr_3$ was abnormally high. That is ascribed to changes in binding energy and dielectric properties after doping of Ba^{2+}. Doping with Ba^{2+} ions significantly enhanced the polarization, while the polarization decreased for dopant Mg^{2+}, Ca^{2+}, and Sr^{2+} ions. That is attributed to the reduction of dielectric constant.

Crystallinity is a crucial factor for enhancing internal polarization and dielectric property. The polarization direction is closely related to crystallization because crystal orientation has a great impact on piezoelectricity and ferroelectricity. Therefore, the synthesis of interfacial charged materials with high crystallinity is particularly helpful to enhance their polarization. The Czochralski method is a traditional method for synthesizing bulk single crystals. As for nanoscale materials, the synthesis strategy requires more in-depth investigation. Wang et al.[77] used a vapor-liquid-solid process to grow ZnO nanowires on c plane-oriented α-Al_2O_3 substrate (Figure 5B). Due to the consistent crystal orientation on the c axis, the ZnO nanowires exhibit excellent interfacial charging property and can work as piezoelectric nanogenerator (PENG). In addition, the dimensionality of nanoscale interfacial charged materials also has an impact on their polarization. The nanomaterials can be synthesized into one-, two-, and three-dimensional structures in a controlled manner (such as hydrothermal method) to regulate their interfacial charging property. For example, in ZnO nanomaterials, the polarization of nanosheets is superior to that of nanowires, while the polarization of nanowires and nanopillars in $BaTiO_3$ materials is better.[102] Additionally, the mechanical-to-electrical energy conversion efficiency of vertically aligned PZT nanorod arrays differs from that of laterally grown PZT nanofibers.[110,111] In the future, the relationships between crystallinity and dielectric property and polarization need to be further investigated.
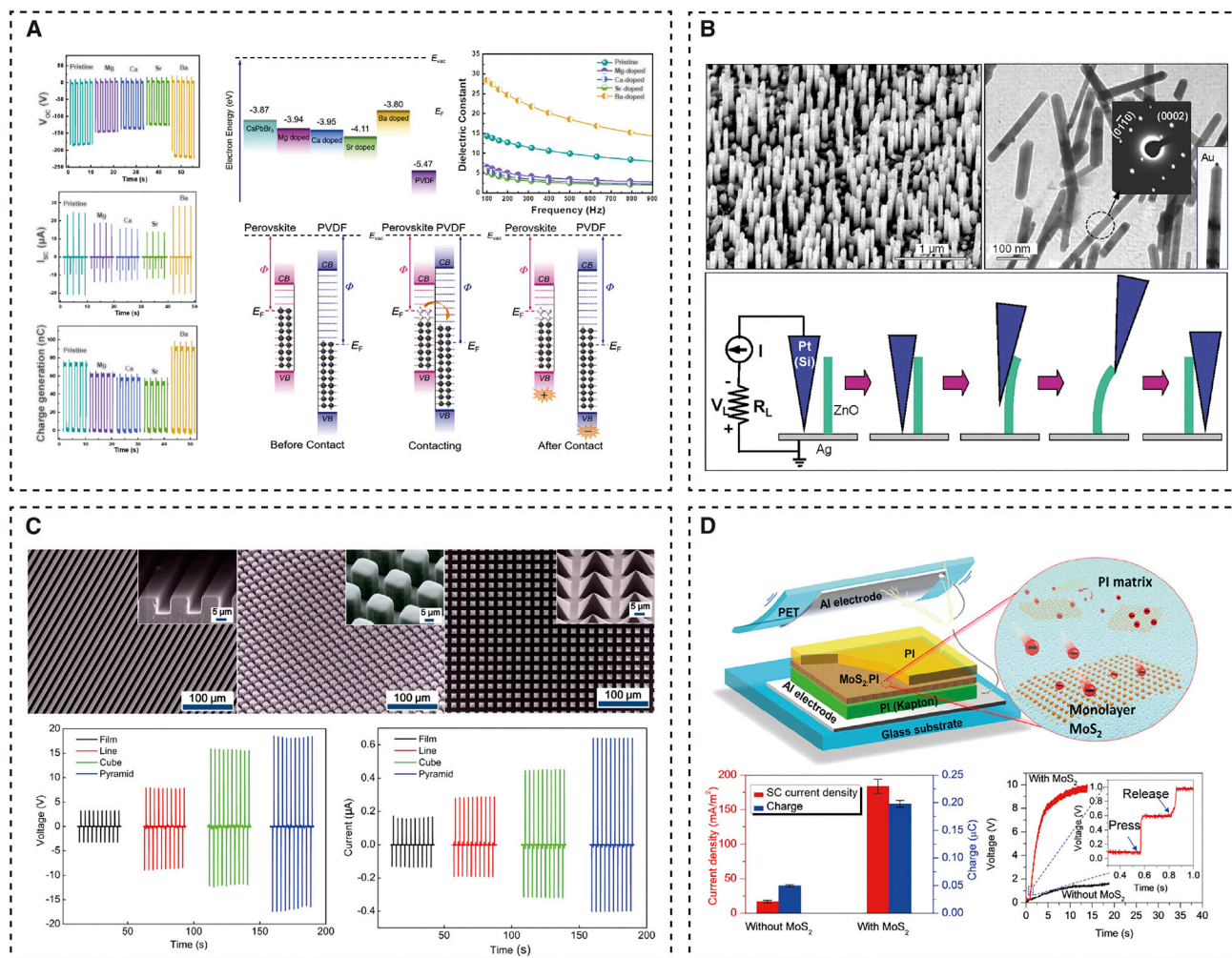
Figure 5. Optimization of interfacial charging

(A) The effects of different alkaline earth metal dopants on output and dielectric constant of CsPbBr$_3$. Reproduced with permission from Wang et al.[107] Copyright 2020, Elsevier.

(B) Morphology and working schematic of aligned ZnO nanowires. Reproduced with permission from Wang et al.[77] Copyright 2006, The American Association for the Advancement of Science.

(C) PDMS surface morphologies with different patterns and their corresponding output plots. Reproduced with permission from Fan et al.[108] Copyright 2012, American Chemical Society.

(D) Sketch and output of device composed of MoS$_2$ monolayer nanosheets and Kapton film. Reproduced with permission from Wu et al.[109] Copyright 2017, American Chemical Society.

Constructing composites from materials with strong polarization and high dielectric constant can promote interfacial charging. For example, inorganic dielectric particles are well dispersed in flexible PVDF and PDMS to enhance interfacial charging of PVDF and PDMS. This strategy can be achieved by vapor deposition, spin-coating, solution casting technology, and so on.[111] PVDF is a widely used flexible piezoelectric material, whereas its internal polarization is relatively weak. By adding dielectrics into PVDF matrix, the as-fabricated PVDF composites display improved polarization and good flexibility.[112] For example, MWCNT and some carbon-based materials can greatly promote the polarization of PVDF.[113,114] Chen et al.[93] demonstrated that the interfacial charge density and charge transfer of PDMS are highly related to their relative dielectric constants. They embedded various dielectric nanoparticles (for example, TiO$_2$) into PDMS porous films to improve the dielectric

CellPress
OPEN ACCESS

property of PDMS. They found that PDMS film embedded with $SrTiO_3$ showed the highest relative dielectric constant (~300), which increased the output power by five times compared with pure PDMS films.

Strengthening interfacial charge capture

Interfacial charge capture is responsible for charge retention and transfer at interfaces. In materials for contact electrification, strategies such as selecting suitable materials, surface engineering, introducing intermediate layers, and reducing the thickness of materials have been proposed to strengthen interfacial charge capture. The selection of suitable materials was mentioned earlier based on an empirical table and electron affinity. Also, some methods to strengthen interfacial charge capture in internally polarized materials have been developed. Here, some effective means are discussed.

Increasing the effective surface area directly elevates output voltage of interfacial charged materials for contact electrification. Large contact area at interface promotes the possibility of electron transfer.[115] Engraving micro-nano patterns on contact interface or increasing interfacial roughness helps to enlarge contact area and thus elevate output.[116] The template method can introduce well-arranged and shape-controlled micro-nano patterns at interfaces. Fan et al.[108] synthesized PDMS films with linear, cubic, and pyramidal micro-nano patterns using Si templates and formed a pair of interfacial charged materials with PET (Figure 5C). The PDMS with pyramidal patterns can reach an output of 18 V, while that of PDMS without surface structure is less than 5.0 V. The development of new surface engineering, such as block copolymer self-assembly, is of interest to enhance interfacial charging.[117]

Apart from physical structure, changing the chemical composition of interfaces is also an important means to enhance interfacial charging. By chemical modification, the interface may gain more charges during contact electrification. Fluorine, for example, has strong electronegativity, which can help capture electrons in contact electrification. Feng et al.[118] used polypropylene nanowire arrays and Al film as a pair of interfacial charged materials. Then polypropylene nanowire surface was further modified with fluorinated polymer. The electrons at Al film interface can be effectively captured by fluoropolymer on nanowire when they are in contact, resulting in 1.9 kV high output. Yao et al.[92] investigated how chemical modification of cellulose nanofibrils (CNFs) affects their interfacial charging properties. The interfacial negative charge density of nitro-modified CNFs was 85.8 $\mu C\ m^{-2}$ and the interfacial positive charge density of methyl-modified CNFs was 62.5 $\mu C\ m^{-2}$, which can rival commonly used Kapton films. The nitro- and methyl-modified CNFs can be directly paired into a pair of interfacial charged materials, outputting an average voltage of 8.0 V. Another strategy to change the chemical composition of an interface is to introduce other materials that usually exhibit outstanding electrical properties. Huang et al.[119] introduced dispersed graphene oxides as charge trapping sites in PVDF nanofibers to increase charge storage at interface, thus elevating voltage output. Wu et al.[109] introduced MoS_2 monolayer nanosheet to the interface of Kapton film (Figure 5D), and the peak power density output at the modified interface was 120 times higher than that of pristine Kapton. The high output results from the good electron-receiving property of the MoS_2 monolayer nanosheet. These studies demonstrate the possibility to use other materials with unique properties for strengthening charge capturing at interfaces. At semiconductor-metal/metal oxide contact interfaces, the charge density at an interface can often be restricted by Schottky barriers and p-n junctions. It is then necessary to modulate the chemical composition of semiconductor-metal/metal oxide interface.[120] Screening effect, free charge, and other factors at

metal/semiconductor interfaces should be regulated to maximize the output performance in both internal polarization and contact electrification.

Increasing charge density in air and reducing charge diffusion at interfaces are recently emerging strategies to enhance interfacial charging. The diffusion of charge occurred at the interface into atmosphere, and the interior of the material is one of the bottlenecks to enhance output of interfacial charged materials. To restrain the dissipation and amalgamation of charges at interfaces, a functional interlayer is proposed. This interlayer is embedded between two materials for contact electrification. The functional intermediate layer can enhance interfacial charging by constructing charge storage and conductive layer, or high dielectric constant-induced polarization.[121] From another perspective, external charge injection is conducive to elevating interfacial charge density. Xu et al.[122] proposed a method to increase interfacial charge density by using a floating layer structure and charge pumping. The floating layer was employed to generate electrostatic induction that can achieve an ultra-high interfacial charge density of 1,020 $\mu C\ m^{-2}$. Further, Liu et al.[123] implemented charge excitation using a voltage-multiplying circuit to enhance the charge injection at the interface with high integrality.

The optimization of structure can raise efficiency of interfacial charge utilization. The common construction modes of interfacial charged materials for contact electrification are often vertical contact separation and lateral sliding.[10] Recently, various novel modes have been proposed, such as free-standing powder as interfacial charged materials, and rotating-type mode.[45,124] These constructed modes provide new perspectives for achieving continuous, high-frequency, and efficient contact and separation at material interfaces.

THE MECHANICAL ENERGY THAT INTERFACIAL CHARGED MATERIALS RESPOND TO

As a bridge between the physical world and computer systems, mechanical-responsive intelligent sensors have broad application scenarios in robotics, artificial intelligence, biomedicine, and so on. Interfacial charged materials can scavenge unimpressive mechanical energy in daily life to supply energy for mechanical-responsive intelligent sensors, while converting the signals concealed in mechanical energy into other signals. At present, researchers have developed mechanical-responsive intelligent sensors based on interfacial charged materials in different fields. Their practical applications are briefly discussed below.

The mechanical energy in human body

Our bodies generate thermal, chemical, electrical, and mechanical energy at every moment.[125] Mechanical energy is pivotal in the body, as our breathing, heartbeat, muscle contraction, and other processes are accompanied by mechanical energy output. However, the mechanical energy in the body is usually not well utilized. In addition, the mechanical energy in the body reflects human health and can be used for health monitoring. As already mentioned, interfacial charged materials can effectively convert mechanical energy into electric fields between interfaces. They can finally output current and serve as energy and signal sources for mechanical-responsive intelligent sensors. Therefore, interfacial charged materials are promising building blocks for mechanical-responsive intelligent sensors.

Health diagnostic system of body

Mechanical energy in the body can imply occurrence of diseases. Mechanical-responsive intelligent devices constructed of interfacial charged materials facilitate

monitoring of human health. Among various factors, heart rate is a key concern in clinical medicine. Failure to quickly detect sudden changes in heart rate will give rise to life-threatening and fatal situations in cardiopathic patients.[12] Therefore, the mechanical-responsive intelligent devices that can continuously and accurately monitor heart rate in real time in the body will help treat cardiovascular diseases. Ma et al.[12] utilized a pair of flexible interfacial charged materials consisting of dry-etched PTFE film with nanopillar structured interface and Al film to detect heart rate *in vivo*. Heartbeat motion drives voltage output when PTFE film continuously contacts with Al film and separates from Al film. The PTFE film, Al film, and other involved substrates are mounted on porcine heart to monitor heart rate with 99% accuracy. Pulse is an important signal derived from heartbeat. Continuous monitoring of arterial pulses using pressure sensors mounted on the epidermis is more convenient in comparison with implantable devices.[126] Park et al.[24] developed a pulse sensor using PZT film that was attached to wrist or neck to monitor pulse signal (Figure 6A). The mild mechanical movement of pulse can drive the PZT to polarize and output a voltage signal, enabling the recognition of tiny arterial pulses. Finally, they used a microcontroller and Bluetooth transmitter for wireless signal acquisition.

Respiration is also an indicator for evaluating human health, such as apnea syndrome.[127] Clinical respiratory monitoring methods such as intubation and breathing masks have inconvenienced patients. To overcome that problem, Peng et al.[127] used electrospun nylon 66 (PA 66) nanofibers and polyacrylonitrile (PAN) nanofibers as flexible interfacial charged materials for contact electrification. In this way, they constructed patient-friendly electronic skin that can acquire respiratory signals in the abdomen (Figure 6B). The mechanical movement of skin during respiration acts on the interfacial charged materials. With maximum output of 330 mW m^{-2} and lightweight structure, this electronic skin can evaluate obstructive sleep apnea hypoventilation syndrome during sleep.

Muscle function is indispensable to life, especially that of the aged. Nonetheless, the muscle assessment often highly relies on physician experience, which leads to an urgent need for intelligent sensors that can quantify muscle movement precisely. Wang et al.[130] fabricated a stretchable intelligent device that is able to evaluate muscle functions. This capability is achieved by using silicone rubber with nanopillar structures and parylene-C to realize contact electrification. Muscle contraction causes bending and close contact of the two interfacial charged materials, therefore creating charge separation.

Mechanical assessment of soft tissues and organs paves a way to early diagnosis and treatment of skin diseases. Dagdeviren et al.[131] used PZT nanoribbons to construct mechanical actuator and sensor network to measure elastic modulus of epidermis. The devices are affixed to target skin region and the PZT acts as both actuator and sensor, and the voltage generated under the same actuation conditions changes due to variation of elastic modulus. This study has clinical implications for non-invasive diagnosis of skin disease.

Treatment of disease using mechanical energy in body

In addition to diagnosis based on biomechanical properties, mechanical energy in the body can also act as an energy source to assist in disease treatment. To treat slow heart rate, cardiac pacemakers emit regular electrical pulses that can keep the heart beating. However, the cardiac pacemaker relies on a battery for its energy supply, which is not conducive to long-term implantation. Ouyang et al.[128] used Al and PTFE film as materials for contact electrification to generate voltage output
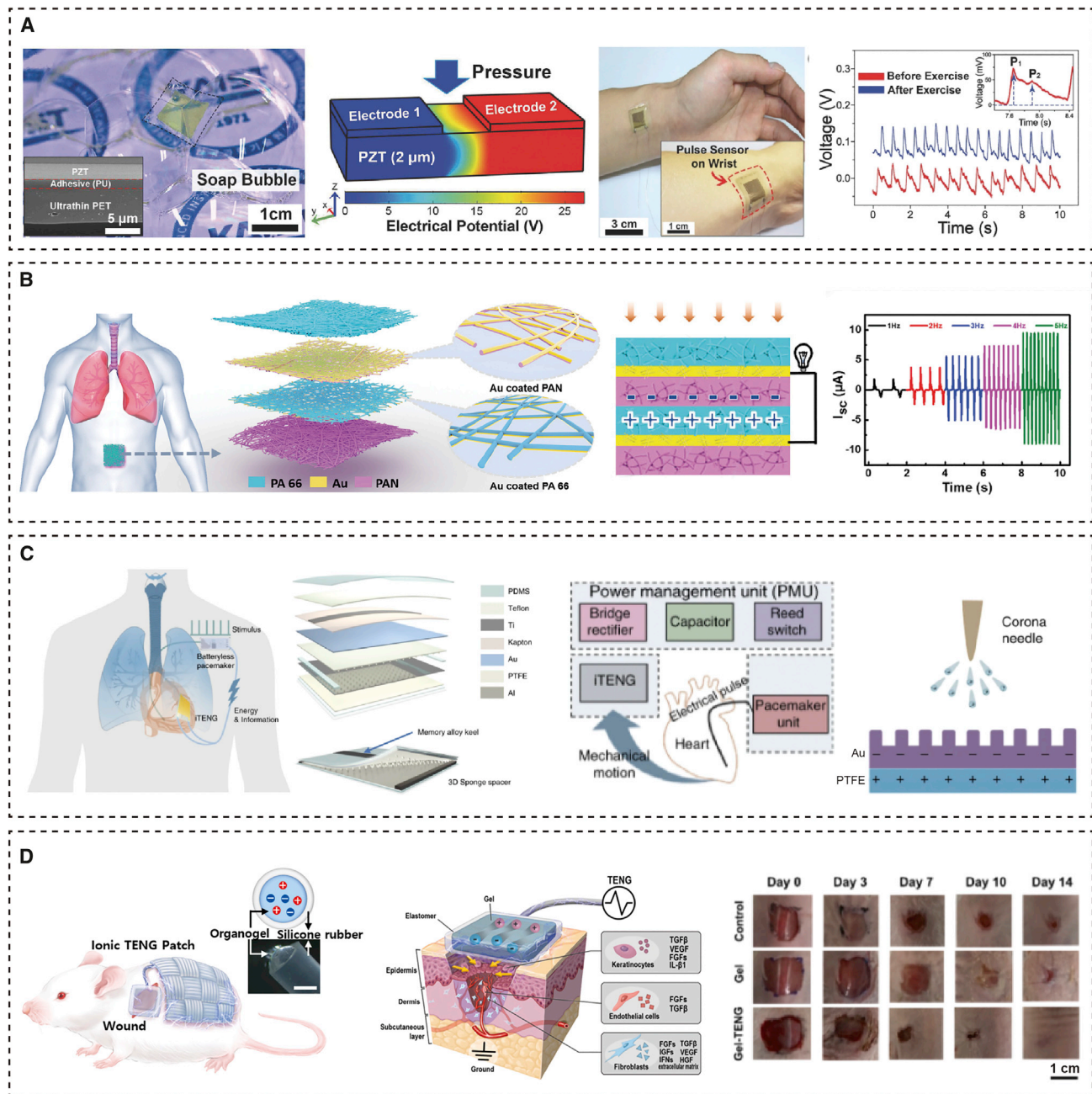
Figure 6. Interfacial charged materials respond to mechanical energy in body

(A) Structure and performance of the pulse sensor film fabricated with PZT. Reproduced with permission from Park et al.[24] Copyright 2017, Wiley-VCH.

(B) Structure and mechanism of PAN and PA 66 coated with Au electrodes to harvest mechanical energy in abdomen during respiration. Reproduced with permission from Peng et al.[127] Copyright 2021, Wiley-VCH.

(C) Schematic illustration of PTFE film and Al film serving as interfacial charged materials to scavenge mechanical energy of heartbeat and sketch of power output enhancement by corona discharge treatment of PTFE. Reproduced with permission from Ouyang et al.[128] Copyright 2019, Springer Nature.

(D) Schematic diagram of electrical stimulation therapy that employs organogel fibers as interfacial charged materials and corresponding treatment outcome. Reproduced with permission from Jeong et al.[129] Copyright 2021, Elsevier.

(Figure 6C). This implantable triboelectric nanogenerator (TENG) produces a maximum output of 65.2 V. Under powered conditions, the energy obtained in each cardiac exercise cycle is sufficient to continuously power the pacemaker. In

this work, the investigators also enhanced interfacial charging using an air discharge strategy, and they used a corona discharge method to increase interfacial charge density of PTFE.

Interfacial charged materials can convert mechanical energy in the body into voltage output. The electrical stimulation can induce a response in cells and realize treatment, such as electrical stimulation therapy. Jeong et al.[129] utilized organogel fibers and skin as interfacial charged materials, and skin-to-gel charge transfer occurred when organogel fibers were in contact with skin. This contact electrification provided electric field to the wound, which can promote rapid wound healing in living animals (Figure 6D). Electrical stimulation is also a powerful tool for neuroprosthesis.[132] Deep brain stimulation can effectively relieve neuropsychiatric disorders such as Parkinson's disease. Nevertheless, commercial brain stimulation devices require frequent battery replacement, posing a risk to the patients' bodies. Hwang et al.[133] used an internally polarized Pb $(In_{1/2}Nb_{1/2})$ O_3-Pb $(Mg_{1/3}Nb_{2/3})$ O_3-PbTiO$_3$ (PIMNT) ferroelectric film to harvest mechanical energy for deep brain stimulation. Body movement of the animal caused a slight bending of PIMNT film to generate current. The high current for stimulation produced a bending movement of the right forelimb in mice. In addition, the electrical stimulation generated by interfacial charged materials has promising applications in therapeutic methods such as promoting osteoblast differentiation.[134–137]

The mechanical-to-electrical energy conversion of interfacial charged materials can also serve as a switch for controlled drug release. Ouyang et al.[138] developed a controllable drug delivery system using interfacial charged materials, the PTFE film and copper rotator. The contact and friction between PTFE film and copper rotator make these two materials negatively and positively charged, respectively. Under an electrical field, the drug carrier polymer undergoes chemical reaction and structural change, resulting in the release of loaded drug. Based on this technology, the patient can control the drug release from a transdermal drug delivery system by tapping. In addition, the generated electrical energy can power the circuit for drug release rate regulation.

The internal electric potential elicited by interfacial charged materials is believed to promote photo-induced electron-hole separation in photocatalysis. Thus, interfacial charged materials also have great potential for enhancing photodynamic therapy that relies on reactive oxygen species.[139] Yu et al.[140] prepared TiO$_2$/BaTiO$_3$/Au multilayer coaxial heterostructured nanorod arrays. After polarization of BaTiO$_3$, which enhanced electron migration from Au to TiO$_2$, the reactive oxygen species produced by TiO$_2$ under ultraviolet (UV)/visible light excitation were significantly increased and could be used to kill bacteria in wounds.

THE ENVIRONMENTAL MECHANICAL ENERGY THAT STIMULATES THE BODY

We live in a physical world where we perceive mechanical stimuli from the external environment. Mechanical stimuli acting on the body make us develop a sense of touch, sound waves into ears lead to a sense of hearing, and some noxious stimuli may give a pain sensation. Perception of the physical world is essential for human survival. However, some patients with diseases and disabilities are unable to perceive environmental stimuli due to neurological damage, which greatly affects their quality of life. The development of intelligent devices to assist in perceiving mechanical energy of external environmental stimuli can help them in their lives and disease treatment.

Tactile sensation helps the body detect pressure, whereas this is impossible for the disabled who lose the sense of touch. In view of this, Shlomy et al.[141] used interfacial charged materials with contact electrification to help restore the sense of touch in mice. They chose PDMS as negatively charged materials and nylon and cellulose acetate butyrate as positively charged materials. All these interfacial charged materials are considered to be biocompatible. The signals generated by interfacial charging are transmitted to normal sensory nerves to form tactile sensations. They assembled and implanted these interfacial charged materials into the plantar hindfoot of mice in which sensation had been blocked. The hindfoot implanted with interfacial charged materials significantly restored tactile sensation and was able to produce a withdrawal response to mechanical stimulation. Chun et al.[142] developed a sensor that responds selectively to pressure and vibration. Its working principle is similar to slow-adapted and fast-adapted mechanoreceptors in human skin, and the sensor produced a sensory neuron-like output signal pattern. $BaTiO_3$ nanoparticles generate interfacial charges when they are subjected to vibrations, which mimics fast-adapting mechanoreceptors and provides energy supply as well. In contrast, reduced graphene oxide flakes mimic slow-adapted mechanoreceptors that respond to static pressure. They performed *in vivo* tests and results showed that the generated electrical signal can stimulate motor nerves in rats to induce muscle contraction.

Hearing is the perception of sound waves mediated by auditory organs. Hearing loss has afflicted many patients, who opt for cochlear implants that convert sound wave into electrical stimulation of auditory nerve. However, reliance on energy supply limits their full utilization. Liu et al.[143] developed a cochlear implant using interfacial charged materials with contact electrification. PTFE film and Ag are interfacial charged materials. Incoming vibrations from acoustic waves cause contact and separation motions that result in voltage output. Changes in frequency of sound waves directly give rise to changes in output voltage, thereby sensing the acoustic signal. On the other hand, the mechanical energy in sound waves can power this device.

THE MECHANICAL ENERGY OF INTERACTIVE DEVICES

Interactive devices are an important part of modern life, such as robots and electronic skins. The process of interaction is usually accompanied by transmission of mechanical energy. Harvesting the interfacial mechanical energy of interactive devices can not only provide energy source for electronic devices but also participate in the interaction process.

Perception system for intelligent robots

Robots are now widely used in industrial production. Sophisticated computational systems, coupled with application of artificial intelligence and machine learning, have made robots behave like people. However, low-level perception like tactile sensation in robots is still hard to establish.[144] Interfacial charged materials have functions of simultaneously achieving energy supply and fast pressure sensing, and the size of materials can be precisely tuned into nanoscale. Thus, a large-scale distributed sensor system is viable for robots.[51,145] Gao et al.[146] combined flexible piezoelectric PVDF polymer with hydrogel piezoresistive sensors to help robots recognize contours. For PVDF, the dynamic strain during touching an object is converted into transient current output, which can reflect the morphology of the object. Jin et al.[147] proposed a composite sensor consisting of a patterned-electrode tactile sensor and a length sensor with gear structure to achieve intelligent perception of robotic manipulators (Figure 7A). They detected the sliding and contact position

CellPress
OPEN ACCESS

by patterned electrodes and sensed the bending angle of the soft actuator. This sensor system is able to sense external mechanical stimuli and the motion of a robotic manipulator.

Human-machine interaction interface

Human-machine interaction interfaces play crucial roles in enabling efficient cooperation between people and the digital world.[149] Human-machine interaction devices, such as smart watches, smart gloves, and smart glasses, can improve the experience of people using electronic devices. Skin, as the largest organ and an excellent interfacial charged material, may play important roles in human-machine interaction interfaces. Many researchers have leveraged the charged nature of skin to realize contact electrification. Chen et al.[148] reported a smart keyboard that is self-powered by interfacial charged materials (Figure 7B). The smart keyboard was affixed with fluorinated ethylene propylene (FEP) that has nanowire surface structure. FEP and human finger skin formed a pair of interfacial charged materials. The contact and separation between FEP and skin during keyboard operation can produce electrical signals. Meanwhile, this smart keyboard can recognize the user's operating habits and thus build a security alert system to identify outsiders. Dhakar et al.[150] used finger skin as an interfacial charged material, and a wearable sensor was therefore developed where the contact separation of the skin and PDMS interface caused charge separation. The static and dynamic position of the finger can be detected, promising direct interaction between intelligent devices and the human body.

Mechanical energy-induced luminescence in interfacial charged materials is also promising for the development of human-machine interaction devices. The generation of electric fields by interfacial charged materials and further excitation of luminescence centers can realize visualized information recording. Electronic signature is one of the important methods of identity verification. Wang et al.[28] designed a pressure sensor for recording electronic signatures based on mechanoluminescence of interfacial charged materials (Figure 7C). They used ZnS particles as interfacial charged materials and doped them with Mn^{2+} as the luminescence center. Under stress, the positive and negative centers of ZnS separate and polarization occurs, and the inner electric field excites carriers in traps to conduction band. Excited carriers then further undergo transition and excite Mn^{2+}, resulting in the emission of orange light. The luminescence intensity is closely related to the pressure, so the dynamics of the signature process can be shown in a visualized way.

The way that human body moves, such as walking and finger movement, may have implications for health assessment and information transfer. For example, the presence of gait abnormalities in the elderly often implies dementia risk and Parkinson's disease. Lin et al.[151] developed interfacial charged materials as insoles for gait abnormality detection. The rubber layer and copper elicit contact electrification, and they generated electrical signals as gait response signals. Hence, the insole can precisely differentiate jumping, stepping, walking, and running in real time. Traditional interfacial charged materials with contact electrification often require intimate contact at the interface. However, it is difficult to make physical contact with the sensor for all human movements. To address this issue, Xi et al.[152] chose the human body and paper as a pair of interfacial charged materials to sense human motion without contact. The paper was first tapped with a Kapton film to make the paper positively charged. When the body moves, an electrical signal is generated because of electrostatic induction. Therefore, the motion state of the body can be determined. Based on a similar principle, Tang et al.[27] developed a non-contact screen sensor using human skin and graphene as a pair of interfacial charged materials (Figure 7D).
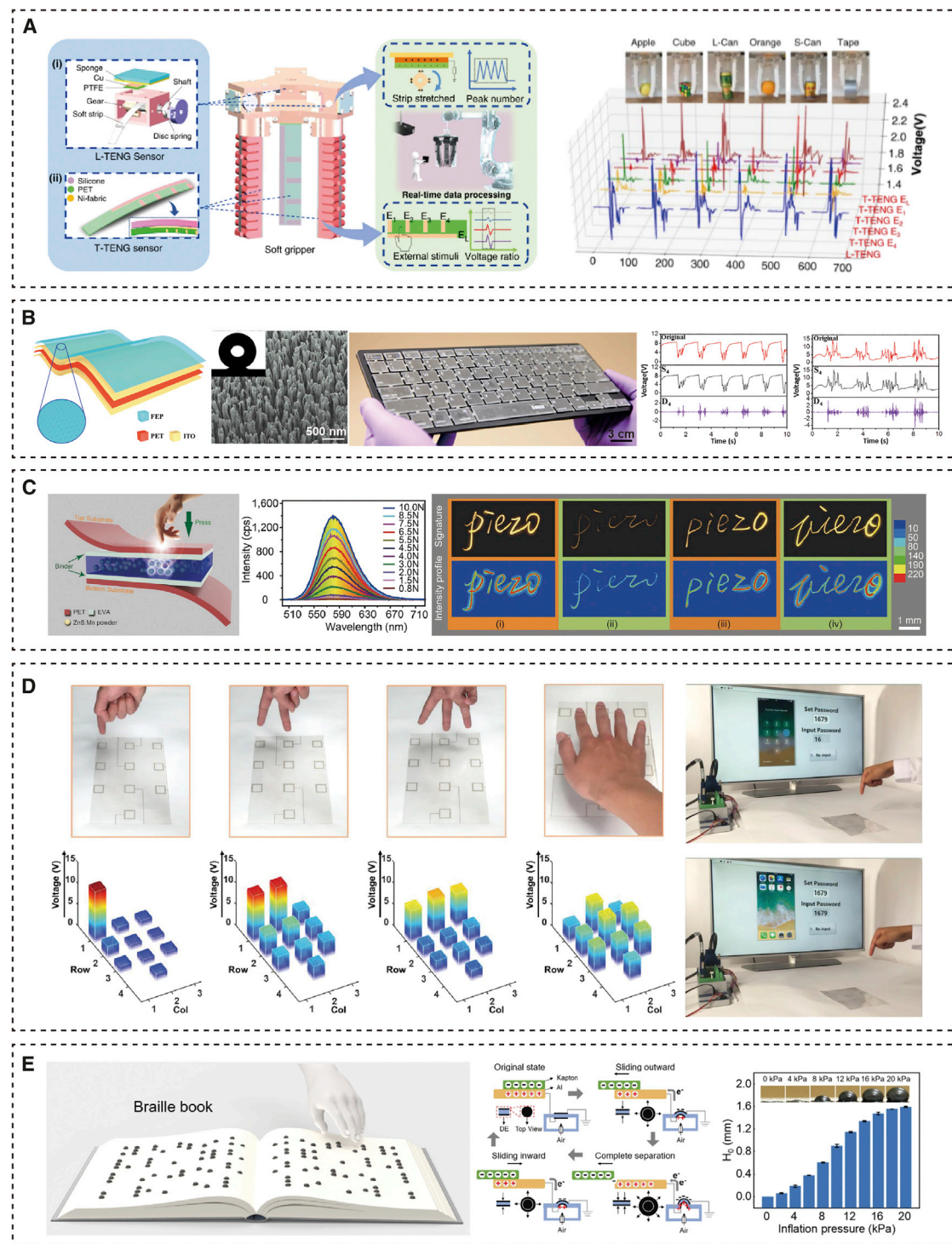
Figure 7. Interfacial charged materials for constructing interactive devices

(A) Structural diagram of sensor on robotic manipulator and voltage signals obtained when robotic manipulator grasps different objects. Reproduced with permission from Jin et al.[147] Copyright 2020, Springer Nature.

(B) Structure of the smart keyboard and voltage signals obtained when two different operators used the keyboard. Reproduced with permission from Chen et al.[148] Copyright 2015, American Chemical Society.

(C) Schematic diagram and performance of mechanoluminescence-based signature pressure sensor. Reproduced with permission from Wang et al.[28] Copyright 2015, Wiley-VCH.

Conventional capacitive screens, such as smartphone screens, can only be used under contact conditions. Interestingly, electrostatic induction between interfacial charged materials is able to break through the above limitation. In the initial state, the fingers are separated from graphene at a certain distance, and some positive charges are induced at the graphene interface. When the finger is close to the graphene interface, more positive charges will gather at the graphene interface to screen the negative charges on the finger, therefore generating an output current signal. This non-contact interfacial charging-based screen provides a novel design for developing next-generation screen sensors.

The development of intelligent human-machine interaction devices with feedback function is important to help people with disabilities. Electrical energy generated from interfacial charging can be further converted into mechanical energy, then the users can feel pressure feedback and obtain relevant information. Braille is a type of writing designed specifically for blind people and consists of raised dots. Qu et al.[55] used the electric field induced at Kapton and Al interfaces to drive the dielectric elastomer to generate mechanical deformation as a refreshable Braille reader (Figure 7E). The interfacial charges can output voltage in excess of 3 kV and current of 2 μA, resulting in obvious deformation of the dielectric elastomer film. Supported by pressurized air inside the cavity, the dielectric elastomer film will be elevated to become a palpable Braille dot. This strategy offers the possibility of developing a portable, refreshable Braille book for blind people.

Similarly, the utilization of interfacial electric fields to power artificial muscles is feasible and interesting.[51,145] The development of artificial muscles is of great importance not only for medicine but also for the development of robotics. Chen et al.[59] developed an artificial muscle driven by interfacial charged materials Kapton film and Al film. The output charges allowed dielectric elastomer to generate 14.5% expansion strain. This system of interfacial charged materials driving dielectric elastomer may have widespread applications in robotics.

Development of a novel intelligent sensor

Recently, the capability of interfacial charged materials as chemical sensors has been stepwise explored. Piezoelectric crystals can be used to construct nano balances by inverse piezoelectric effect (deformation of piezoelectric material under electric field), and the oscillation frequency is measured to detect analyte. The precise binding of the analyte at an interface causes a slight variation in oscillation frequency.[153] The implementation of this process usually requires the modification of antibodies or antigens, allowing the material to specifically capture analytes.

In addition, interfacial charged materials can help construct sensors of gases and liquids. Shen et al.[154] developed a sensor for monitoring automobile exhaust. They chose Al foil and PTFE film as a pair of interfacial charged materials with contact electrification, and the vibration of a car engine will induce an electric field to power the gas sensor. Wang et al.[155] constructed a sensor using interfacial charged materials to sense CO_2 with different relative humidity under static conditions. The sensing range is up to 6,000 ppm. Zhang et al.[156] used interfacial charged materials for humidity or alcohol content detection. They used Al film and PA 66 film/PTFE film as interfacial

(D) Mapping of finger position and distance by non-contact electrostatic induction at graphene and skin interfaces. Reproduced with permission from Tang et al.[27] Copyright 2020, Wiley-VCH.

(E) Schematic diagram and deformation of electronic Braille book powered by interfacial charged materials. Reproduced with permission from Qu et al.[55] Copyright 2021, Wiley-VCH.
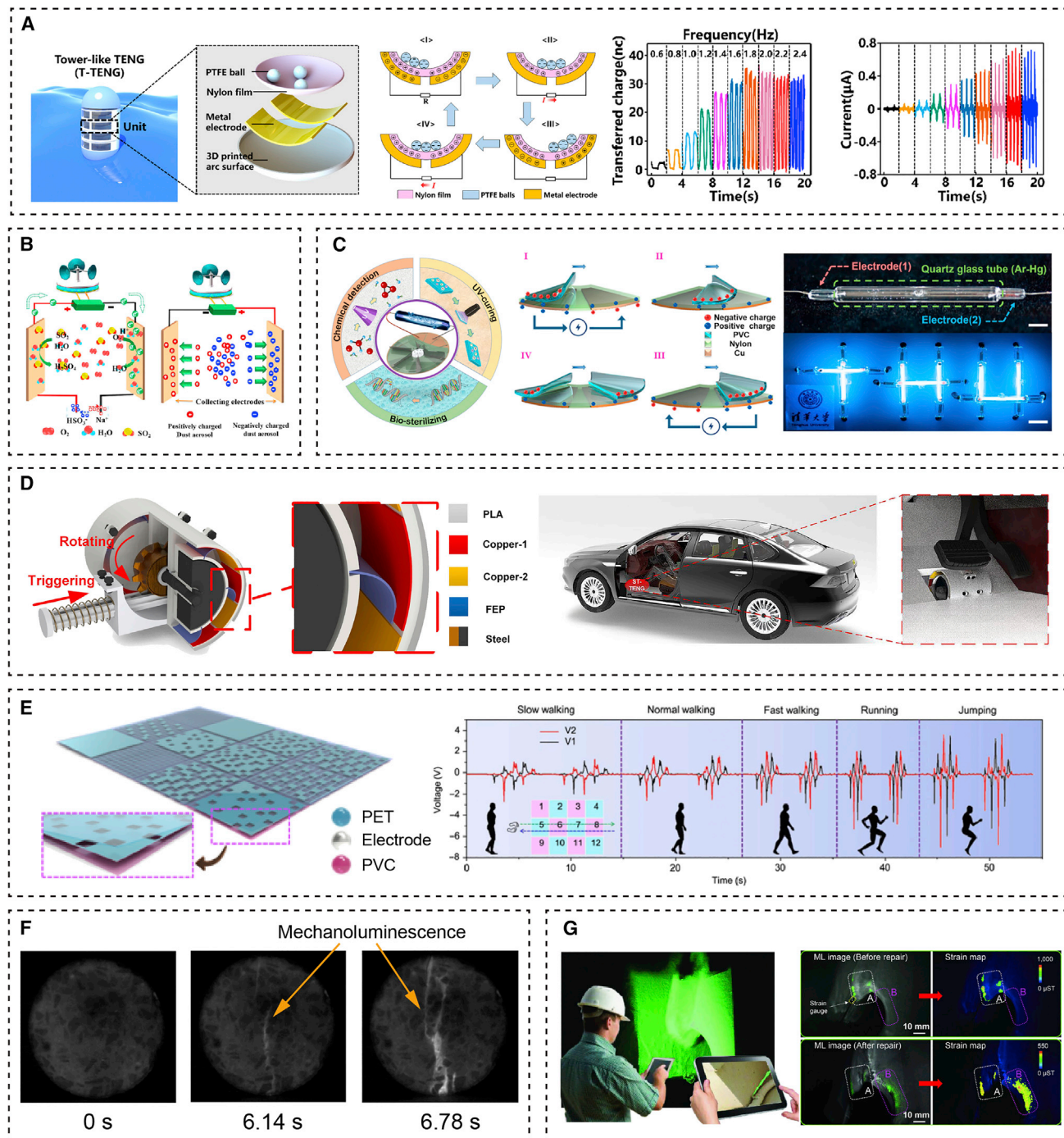
Figure 8. Interfacial charged materials for harvesting mechanical energy in smart city

(A) Working principle and output of PTFE ball and nylon film scavenging wave energy of seawater. Reproduced with permission from Xu et al.[159] Copyright 2019, American Chemical Society.

(B) Schematic diagram of high voltage generation by interfacial charged materials for catalytic oxidation of SO_2 and electrostatic adsorption of dust particles. Reproduced with permission from Chen et al.[160] Copyright 2015, Elsevier.

(C) Schematic diagram of ultraviolet light generation by interfacial charged materials and its applications in air sterilization. Scale bars, 10 mm (top) and 20 mm (bottom). Reproduced with permission from Wang et al.[161] Copyright 2020, Elsevier.

(D) Structural diagram of FEP film and copper constructing petal sensor to sense operating habits of drivers. Reproduced with permission from Xie et al.[162] Copyright 2020, Elsevier.

charged materials for contact electrification, and the output voltage was significantly increased after using etched Al foil as the electrode. The voltage generated by contact electrification also changes when different concentrations of ethanol solution are added dropwise to the PTFE surface. Chen et al.[157] devised a liquid sensor by using the inner wall of a PTFE capillary as interfacial charged materials and double-helical Al foil as the electrode. They achieved micro liquid sensing by using this sensor.

MECHANICAL ENERGY IN SMART CITY

Cities are the main gathering place of modern population. Due to the high-density population, modern cities are often accompanied by numerous problems such as environmental pollution, insufficient energy supply, traffic congestion, and decreasing living comfort. With the advent of the Internet of Things and the 5G era, smart city networks hold the promise of solving the aforementioned problems, and intelligent sensors are important components of smart city networks. Due to the unique mechanical-to-electrical energy conversion, intelligent sensors based on interfacial charged materials have become a hot topic of interest for researchers.

Sustainable energy and environmental protection

With the increasing urbanization, the demand for energy is growing exponentially. Electricity is indispensable to urban living and industrial production and is mainly provided by thermal power generation. However, since coal combustion is non-renewable and also generates air and water pollution, there is a great need to develop alternative modes of power generation. Nature contains abundant renewable sources of energy, such as mechanical energy in wind and ocean. Scavenging the ubiquitous mechanical energy in nature and reducing the reliance on traditional power generation technologies are favorable.

As clean and renewable energy sources, wind-driven generators have been developed worldwide to complement thermal power generation. Given this, Zhao et al.[158] used polyester, Kapton film, nickel film, and copper film to weave a flag to harvest wind energy. The contact electrification of nickel and Kapton film bring positive and negative charges, thus generating voltage output to power weather sensing systems. The development of ocean energy (e.g., wave energy) has received tremendous attention. Despite decades of research on wave energy, there are still many obstacles, such as the high cost of electromagnetic generators.[45] Given this, Xu et al.[159] developed a tower-shaped generator suspended in seawater that can scavenge wave energy from any direction (Figure 8A). This generator consists of hemispherical nylon film wrapped around PTFE balls, and then electrodes are attached to the outside. As the waves lap against the generator, the PTFE balls roll back and forth inside the nylon film cavity. In the process of contacting and rolling, the interfaces between PTFE and nylon film are negatively and positively charged respectively, and the relative movement between PTFE and nylon film form an electric field. On this basis, the wave energy of seawater is transformed into electricity, and the output increased with increase of rolling frequency. Moreover, the layer number has a great effect on output performance.

(E) The diagram and signal plots of PVC and PET films for constructing smart floor mat. Reproduced with permission from Shi et al.[163] Copyright 2020, Springer Nature.

(F) Real-time mapping of crack in concrete based on mechanoluminescence. Reproduced with permission from Timilsina et al.[164] Copyright 2017, Elsevier.

(G) Schematic diagram of crack extension detection of buildings based on mechanoluminescence and computer vision. Reproduced with permission from Liu et al.[26] Copyright 2019, Wiley-VCH.

Apart from energy depletion, environmental pollution is another important challenge in cities. Air pollution, especially dust and harmful gases, greatly threatens human health. Electrostatic dust removal has been widely used in industry, where dust in gases is separated in a high-voltage electrostatic field. The contact electrification and separation of interfacial charged materials can generate high voltage and electrostatic energy at interfaces, which can act as a high-voltage electrostatic field that discharges in air. Chen et al.[160] developed an air-driven air purification system for sulfur dioxide (SO_2) and dust removal (Figure 8B). The power supply system is a rotating structure composed of interfacial charged materials. The air passing by drives the rotator to rotate, and frictional motion occurs between interfacial charged materials and results in interfacial charging and electrostatic induction. The output voltage can reach 300 V. That voltage can electrocatalytically oxidize SO_2 and adsorb the formed dust. Drinking water safety is becoming a global challenge. Ozone is usually recognized as a green and high-efficiency disinfectant. However, ozone preparation such as UV irradiation usually requires an ultra-high-voltage power supply of more than thousands of volts. Lei et al.[165] developed a method for efficient ozone production using interfacial charged materials under mild conditions. They constructed a rotating power generator, where rotation causes contact electrification and a strong electric field between the copper electrode and two polymers with maximum transient voltage of over 30.7 kV. This high voltage can generate air-breakdown discharge and ozone. The obtained ozone degrades 97.6% of rhodamine B at a concentration of 5 ppm within 20 min, while it is also effective in killing microorganisms in water. Likewise, Wang et al.[161] used a high voltage driven by interfacial charged materials to generate UV light via glow reaction as a mobile UV light source that can be used for air sterilization (Figure 8C).

Intelligent transportation

Transportation is the key link of a smart city network. Intelligent traffic volume sensors can measure real-time traffic flow in transportation systems. Zhang et al.[166] developed a traffic volume sensor that possesses a rotating disc structure that was constructed from the interfacial charged materials PTFE film and Al film. The nanostructure of films enlarges their contact areas. The wind energy generated by moving vehicles drives the rotator to rotate, and the PTFE and Al films inside the device rub together to produce interfacial charges. The output is proportional to rotation speed within a certain range and can be used to monitor speed of airflow and thus determine the speed of a vehicle. Lin et al.[167] placed devices directly on the ground and used the time difference of vehicles passing through two devices to determine speed. They used a wet chemical approach to grow ZnO nanowires on a flexible PDMS substrate. Under the effect of vertical stress, ZnO polarizes and generates charges at interfaces. The output voltage generated between electrodes can reach 8.0 V. When a vehicle passes by, the voltage can be generated without an external power source to determine speed of vehicle.

Automobiles are the core of urban transportation. In recent years, smart cars have developed significantly, including assisted driving systems, exhaust sensors, and safety sensors. Due to the response to mechanical energy, interfacial charged materials can also be involved in the development of smart cars. Pedals are an important operational component that can monitor driving habits. Xie et al.[162] developed an intelligent sensor placed under the pedal of a car where the driver can generate corresponding voltage signals by stepping on the pedal during driving (Figure 8D). They used FEP film and copper electrodes for contact electrification. This sensor can convert the random triggering motion of foot pedaling into continuous rotational motion, thus causing friction between the FEP film and copper electrodes

CellPress
OPEN ACCESS

and generating voltage output. In this way, the frequency of a driver stepping on the gas pedal and brake can be obtained, and this frequency varies with the road conditions. This sensor can monitor and analyze driving behaviors and help establish driverless systems.

Smart home and building inspection

The rapid development of the Internet of Things has made it possible for every item of furniture and even every brick in our homes to become part of a sensing unit, thereby forming a sensing network in a smart home. Mechanical-responsive intelligent sensors can be deployed in a house and are connected wireless to enable intelligent sensing in the smart home. Shi et al.[163] used screen printing technology to fabricate a smart floor mat that includes contact arrays of the interfacial charged materials PET and polyvinyl chloride (PVC) films. This mat harvests mechanical energy applied to the floor by humans (Figure 8E). Deep-learning-based data analysis allows identification of gait patterns from generated electrical signals. Smart toilets provide another viable method of human health monitoring. Zhang et al.[168] developed an intelligent toilet using interfacial charged materials as pressure sensors. The pressure sensor installed on the toilet can obtain pressure distribution and biometric information. This toilet combined with deep learning can correctly identify the user with an accuracy of over 90%.

Building safety is a key concern that must be addressed in smart homes. Diagnosis of engineered structures (e.g., load-bearing elements of building) is a crucial technology. The crack tracking is essential in monitoring the state of concrete structures. So far, various techniques for visualization of static crack or crack motion in building structures, including guided wave imaging, have been developed. However, these methods require complex measurement equipment and analysis processes that are not conducive to practical applications.[164] When an interfacial charged material is doped with a luminescence center, the internal luminescence center will be excited and emit luminescence of corresponding wavelength under pressure. Importantly, the intensity of luminescence depends on the pressure exerted on the material. This excellent mechanoluminescence property of interfacial charged materials has the potential for visualization of static and dynamic cracks. Thus far, research on structural damage diagnosis using interfacial charged materials has mostly focused on $SrAl_2O_4$ doped with Eu^{2+}, Ln^{3+}, or other ions because of the strong intensity and long decay time of its mechanoluminescence.[164] Back in 2002, Sohn et al.[169] conducted an extensive dynamic visualization study of crack extension in fractured ceramics using $SrAl_2O_4$:Eu dense solid mixed with epoxy resin. Li et al.[170] developed mechanoluminescent sensors using $SrAl_2O_4$:Eu thin film coatings for predicting fractures in reinforced concrete structures. From the mechanoluminescence images of concrete surface, the location of mechanoluminescence was found to be consistent with the location of cracks caused by increased loading. Timilsina et al.[164] also employed $SrAl_2O_4$:Eu,Dy to study the dynamics of concrete cracks (Figure 8F). Their results indicate that cracks can be precisely monitored and further predicted using mechanoluminescent sensors of interfacial charged materials. Zhang et al.[171] proposed a strategy that combines computer vision and machine learning to realize crack visualization. In the future, this method can be combined with mechanoluminescence materials to achieve intelligent detection of cracks in building structures (Figure 8G).[26] In addition to internal polarization, voltages generated by contact electrification can also give rise to strong mechanoluminescence, which is also promising for visualization of stress distribution in smart homes.[68]

SUMMARY AND OUTLOOK

The charge separation and interfacial charging due to mechanical energy are interesting phenomena. Researchers have developed various interfacial charged materials that generate electrical energy output in response to mechanical energy, thus enabling the mechanical-to-electrical energy or to other energy conversion. From the perspectives of physics and chemistry, many strategies have been proposed to enhance interfacial charging, such as modulating the dielectric properties, polarizability, and surface engineering. Due to high sensitivity to mechanical energy, transient high voltage output, simplicity, and low cost of fabrication, interfacial charged materials have been widely used in self-powered intelligent sensing, such as electronic skins, tactile sensors, and nanogenerators. The all-weather output characteristics and pressure linear response make these materials promising to overcome power supply challenges encountered by current mechanical-responsive intelligent sensors. Interfacial charging can further motivate the development of the Internet of Things and other fields. Although interfacial charged materials have been extensively studied as intelligent sensors and nanogenerators, and the output performance has been greatly improved in the past decade, there are still many challenges in interfacial charged materials to be resolved.

First, the incompatibility between the structure/composition of interfacial charged materials and working environment needs to be fully addressed. Some materials with strong interfacial charging tend to be rigid or toxic, such as ferroelectric ceramics. The rigidity and toxicity would be detrimental to their utilization as a flexible intelligent sensor that is attached to skin or implanted inside the body. Moreover, complex external environments will greatly reduce the efficiency of interfacial charging. For example, elevated humidity will reduce the electron transfer between interfaces, and changes in temperature will affect the internal polarization. Those drawbacks require development of interfacial charged materials that are flexible, biocompatible, and highly resistant to interference in different environments. For example, molecular ferroelectric thin films exhibit good flexibility, biocompatibility, and interfacial charging properties.[83] Also, they can achieve precise self-assembly. Thus, molecular ferroelectric thin films have rosy application prospects in biomedical, microelectronics, and many other fields.[172]

Second, the sensing performance of interfacial charged materials still urgently needs to be optimized. Due to the limited mechanical deformation range and displacement range of interfacial charged materials, their pressure responses are confined to a narrow range. For example, piezoelectric materials are rigid and are therefore less likely to undergo a huge mechanical deformation. Compared with conventional capacitive and resistive sensors, the resolution and sensitivity of interfacial charged materials for sensing are still inferior. Meanwhile, the inherent high resistance of interfacial charged materials also limits the output of electrical energy, so how to minimize the loss of electrical energy is an important issue as well. The output of current interfacial charged materials is still insufficient to power high-powered machines. Theoretical simulation and big data analysis may be helpful for developing new interfacial charged materials with high performance. Studies on contact electrification mechanisms will also promote practical applications of interfacial charged materials. Understanding exactly how electrons, ions, and other microscopic particles transfer at interfaces is expected to further increase the difference in interfacial charge distribution and reduce energy loss. Stronger contact electrification may have applications in areas such as renewable energy generation, self-powered intelligent devices, and multi-mode human-machine interaction.

Finally, since interfacial charged materials output transient currents, they often require external storage devices (e.g., external capacitors) to store the generated electrical energy. That will lead to redundancy and hysteresis in electrical energy output and signal acquisition. Also, the coordination of power supply and sensing is not well realized. Thus, circuit design can also motivate the development of interfacial charged materials.

In the future, the development of a new generation of interfacial charged materials optimized in all aspects of performance is inevitable for their practical applications. It appeals to efforts from multiple disciplines, such as chemistry, materials science, and electronics. Further, the use of interfacial charged materials for other energy conversion processes, such as mechanical energy, light energy, chemical energy, thermal energy, and even magnetic field energy, to expand the response modes and application scenarios of intelligent devices is also important to their future prospects.

AUTHOR CONTRIBUTIONS

Conceptualization, W.W., J.T., and Q.Y.; investigation, H.X., L.Z., and Y.W.; writing – original draft, W.W.; writing – review and editing, J.T., H.X., L.Z., and Y.W.; funding acquisition, Q.Y. and J.T.; supervision, Q.Y. and J.T.

DECLARATION OF INTERESTS

The authors declare no competing interests.

REFERENCES

1. Hung, L.-L. (2022). Intelligent sensing for Internet of things systems. J. Internet Technol. 23, 185–191.

2. Zhao, X., Askari, H., and Chen, J. (2021). Nanogenerators for smart cities in the era of 5G and Internet of Things. Joule 5, 1391–1431. https://doi.org/10.1016/j.joule.2021.03.013.

3. He, F., You, X., Wang, W., Bai, T., Xue, G., and Ye, M. (2021). Recent progress in flexible microstructural pressure sensors toward human–machine interaction and healthcare applications. Small Methods 5, 2001041. https://doi.org/10.1002/smtd.202001041.

4. Yang, S., Ding, K., Wang, W., Wang, T., Gong, H., Shu, D., Zhou, Z., Jiao, L., Cheng, B., and Ni, Y. (2022). Electrospun fiber-based high-performance flexible multi-level micro-structured pressure sensor: design, development and modelling. Chem. Eng. J. 431, 133700. https://doi.org/10.1016/j.cej.2021.133700.

5. Lei, H., Chen, Y., Gao, Z., Wen, Z., and Sun, X. (2021). Advances in self-powered triboelectric pressure sensors. J. Mater. Chem. 9, 20100–20130. https://doi.org/10.1039/d1ta03505c.

6. Liu, L., Guo, X., Liu, W., and Lee, C. (2021). Recent progress in the energy harvesting technology—from self-powered sensors to self-sustained IoT, and new applications.

Nanomaterials 11, 2975. https://doi.org/10.3390/nano11112975.

7. Jiao, P. (2021). Emerging artificial intelligence in piezoelectric and triboelectric nanogenerators. Nano Energy 88, 106227. https://doi.org/10.1016/j.nanoen.2021.106227.

8. Huang, X., Wang, L., Wang, H., Zhang, B., Wang, X., Stening, R.Y.Z., Sheng, X., and Yin, L. (2020). Materials strategies and device architectures of emerging power supply devices for implantable bioelectronics. Small 16, 1902827. https://doi.org/10.1002/smll.201902827.

9. Zhou, H., Lai, J., Zheng, B., Jin, X., Zhao, G., Liu, H., Chen, W., Ma, A., Li, X., and Wu, Y. (2022). From glutinous-rice-inspired adhesive organohydrogels to flexible electronic devices toward wearable sensing, power supply, and energy storage. Adv. Funct. Mater. 32, 2108423. https://doi.org/10.1002/adfm.202108423.

10. Wu, Z., Cheng, T., and Wang, Z.L. (2020). Self-powered sensors and systems based on nanogenerators. Sensors 20, 2925. https://doi.org/10.3390/s20102925.

11. Goertzel, T. (2014). The path to more general artificial intelligence. J. Exp. Theor. Artif. Intell. 26, 343–354. https://doi.org/10.1080/0952813x.2014.895106.

12. Ma, Y., Zheng, Q., Liu, Y., Shi, B., Xue, X., Ji, W., Liu, Z., Jin, Y., Zou, Y., An, Z., et al. (2016). Self-powered, one-stop, and multifunctional implantable triboelectric active sensor for real-time biomedical monitoring. Nano Lett. 16, 6042–6051. https://doi.org/10.1021/acs.nanolett.6b01968.

13. Zhang, D., Wang, D., Xu, Z., Zhang, X., Yang, Y., Guo, J., Zhang, B., and Zhao, W. (2021). Diversiform sensors and sensing systems driven by triboelectric and piezoelectric nanogenerators. Coord. Chem. Rev. 427, 213597. https://doi.org/10.1016/j.ccr.2020.213597.

14. Shao, Y., Shen, M., Zhou, Y., Cui, X., Li, L., and Zhang, Y. (2021). Nanogenerator-based self-powered sensors for data collection. Beilstein J. Nanotechnol. 12, 680–693. https://doi.org/10.3762/bjnano.12.54.

15. McCarty, L.S., and Whitesides, G.M. (2008). Electrostatic charging due to separation of ions at interfaces: contact electrification of ionic electrets. Angew. Chem. Int. Edit. 47, 2188–2207. https://doi.org/10.1002/anie.200701812.

16. Trolier-McKinstry, S. (2008). Crystal chemistry of piezoelectric materials. In Piezoelectric and Acoustic Materials for Transducer Applications (Springer US).

17. Li, M., Lu, H.-W., Wang, S.-W., Li, R.-P., Chen, J.-Y., Chuang, W.-S., Yang, F.-S., Lin, Y.-F.,

Chen, C.-Y., and Lai, Y.-C. (2022). Filling the gap between topological insulator nanomaterials and triboelectric nanogenerators. Nat. Commun. *13*, 938. https://doi.org/10.1038/s41467-022-28575-3.

18. Jiang, Z., Tan, X., and Huang, Y. (2022). Piezoelectric effect enhanced photocatalysis in environmental remediation: state-of-the-art techniques and future scenarios. Sci. Total Environ. *806*, 150924. https://doi.org/10.1016/j.scitotenv.2021.150924.

19. Wen, J., He, H., Niu, C., Rong, M., Huang, Y., and Wu, Y. (2022). An improved equivalent capacitance model of the triboelectric nanogenerator incorporating its surface roughness. Nano Energy *96*, 107070. https://doi.org/10.1016/j.nanoen.2022.107070.

20. Wu, C., Wang, A.C., Ding, W., Guo, H., and Wang, Z.L. (2019). Triboelectric nanogenerator: a foundation of the energy for the new era. Adv. Energy Mater. *9*, 1802906. https://doi.org/10.1002/aenm.201802906.

21. Li, Z., Cui, Y., and Zhong, J. (2021). Recent advances in nanogenerators-based flexible electronics for electromechanical biomonitoring. Biosens. Bioelectron. *186*, 113290. https://doi.org/10.1016/j.bios.2021.113290.

22. Wang, W., Pang, J., Su, J., Li, F., Li, Q., Wang, X., Wang, J., Ibarlucea, B., Liu, X., Li, Y., et al. (2022). Applications of nanogenerators for biomedical engineering and healthcare systems. InfoMat *4*, e12262. https://doi.org/10.1002/inf2.12262.

23. Wang, N., Liu, Y., Ye, E., Li, Z., and Wang, D. (2022). Control methods and applications of interface contact electrification of triboelectric nanogenerators: a review. Mater. Res. Lett. *10*, 97–123. https://doi.org/10.1080/21663831.2022.2026513.

24. Park, D.Y., Joe, D.J., Kim, D.H., Park, H., Han, J.H., Jeong, C.K., Park, H., Park, J.G., Joung, B., and Lee, K.J. (2017). Piezoelectric sensors: self-powered real-time arterial pulse monitoring using ultrathin epidermal piezoelectric sensors (adv. Mater. 37/2017). Adv. Mater. *29*. adma.201770272. https://doi.org/10.1002/adma.201770272.

25. Li, T., Zou, J., Xing, F., Zhang, M., Cao, X., Wang, N., and Wang, Z.L. (2017). From dual-mode triboelectric nanogenerator to smart tactile sensor: a multiplexing design. ACS Nano *11*, 3950–3956. https://doi.org/10.1021/acsnano.7b00396.

26. Liu, L., Xu, C.-N., Yoshida, A., Tu, D., Ueno, N., and Kainuma, S. (2019). Scalable elasticoluminescent strain sensor for precise dynamic stress imaging and onsite infrastructure diagnosis. Adv. Mater. Technol. *4*, 1800336. https://doi.org/10.1002/admt.201800336.

27. Tang, Y., Zhou, H., Sun, X., Diao, N., Wang, J., Zhang, B., Qin, C., Liang, E., and Mao, Y. (2020). Triboelectric touch-free screen sensor for noncontact gesture recognizing. Adv. Funct. Mater. *30*, 1907893. https://doi.org/10.1002/adfm.201907893.

28. Wang, X., Zhang, H., Yu, R., Dong, L., Peng, D., Zhang, A., Zhang, Y., Liu, H., Pan, C., and Wang, Z.L. (2015). Dynamic pressure mapping of personalized handwriting by a flexible sensor matrix based on the mechanoluminescence process. Adv. Mater. *27*, 2324–2331. https://doi.org/10.1002/adma.201405826.

29. Chandra, B.P., Chandra, V.K., Jha, P., Pateria, D., and Baghel, R.N. (2016). Is the fracto-mechanoluminescence of ZnS:Mn phosphor dominated by charged dislocation mechanism or piezoelectrification mechanism? Luminescence *31*, 67–75. https://doi.org/10.1002/bio.2924.

30. Li, F. (2022). Breaking symmetry for piezoelectricity. Science *375*, 618–619. https://doi.org/10.1126/science.abn2903.

31. Chandra, B.P., Tiwari, S., Ramrakhiani, M., and Ansari, M.H. (1991). Mechanoluminescence in centrosymmetric crystals. Cryst. Res. Technol. *26*, 767–781. https://doi.org/10.1002/crat.2170260617.

32. Park, D.S., Hadad, M., Riemer, L.M., Ignatans, R., Spirito, D., Esposito, V., Tileli, V., Gauquelin, N., Chezganov, D., Jannis, D., et al. (2022). Induced giant piezoelectricity in centrosymmetric oxides. Science *375*, 653–657. https://doi.org/10.1126/science.abm7497.

33. Yang, M.-M., Luo, Z.-D., Mi, Z., Zhao, J., E, S.P., and Alexe, M. (2020). Piezoelectric and pyroelectric effects induced by interface polar symmetry. Nature *584*, 377–381. https://doi.org/10.1038/s41586-020-2602-4.

34. Gao, W., Zhu, Y., Wang, Y., Yuan, G., and Liu, J.-M. (2020). A review of flexible perovskite oxide ferroelectric films and their application. J. Materiomics *6*, 1–16. https://doi.org/10.1016/j.jmat.2019.11.001.

35. Xu, C., Zi, Y., Wang, A.C., Zou, H., Dai, Y., He, X., Wang, P., Wang, Y.-C., Feng, P., Li, D., and Wang, Z.L. (2018). On the electron-transfer mechanism in the contact-electrification effect. Adv. Mater. *30*, 1706790. https://doi.org/10.1002/adma.201706790.

36. Ren, X. (2004). Large electric-field-induced strain in ferroelectric crystals by point-defect-mediated reversible domain switching. Nat. Mater. *3*, 91–94. https://doi.org/10.1038/nmat1051.

37. Salmani-Rezaie, S., Ahadi, K., Strickland, W.M., and Stemmer, S. (2020). Order-disorder ferroelectric transition of strained SrTiO$_3$. Phys. Rev. Lett. *125*, 087601. https://doi.org/10.1103/physrevlett.125.087601.

38. McMeeking, R.M., and Landis, C.M. (2002). A phenomenological multi-axial constitutive law for switching in polycrystalline ferroelectric ceramics. Int. J. Eng. Sci. *40*, 1553–1577. https://doi.org/10.1016/s0020-7225(02)00033-2.

39. Kim, S.-W., Kim, J.-K., Kim, H.J., Cao, C.T., Khen Oh, N., Yang, Y., Song, H.-C., Shim, M., Park, H.S., and Baik, J.M. (2022). Output signals control of triboelectric nanogenerator with metal-dielectric-metal configuration through high resistance grounded systems. Nano Energy *95*, 107023. https://doi.org/10.1016/j.nanoen.2022.107023.

40. Liu, J., Goswami, A., Jiang, K., Khan, F., Kim, S., McGee, R., Li, Z., Hu, Z., Lee, J., and Thundat, T. (2018). Direct-current triboelectricity generation by a sliding Schottky nanocontact on MoS$_2$ multilayers. Nat. Nanotechnol. *13*, 112–116. https://doi.org/10.1038/s41565-017-0019-5.

41. Wang, Z.L. (2020). Triboelectric nanogenerator (TENG)—sparking an energy and sensor revolution. Adv. Energy Mater. *10*, 2000137. https://doi.org/10.1002/aenm.202000137.

42. You, J., Shao, J., He, Y., Yun, F.F., See, K.W., Wang, Z.L., and Wang, X. (2021). High-electrification performance and mechanism of a water–solid mode triboelectric nanogenerator. ACS Nano *15*, 8706–8714. https://doi.org/10.1021/acsnano.1c00795.

43. Wang, Z.L., and Wang, A.C. (2019). On the origin of contact-electrification. Mater. Today *30*, 34–51. https://doi.org/10.1016/j.mattod.2019.05.016.

44. Lin, S., Xu, L., Chi Wang, A., and Wang, Z.L. (2020). Quantifying electron-transfer in liquid-solid contact electrification and the formation of electric double-layer. Nat. Commun. *11*, 399. https://doi.org/10.1038/s41467-019-14278-9.

45. Kim, D., Oh, Y., Hwang, B.-W., Jeon, S.-B., Park, S.-J., and Choi, Y.-K. (2016). Triboelectric nanogenerator based on the internal motion of powder with a package structure design. ACS Nano *10*, 1017–1024. https://doi.org/10.1021/acsnano.5b06329.

46. Fu, X., Xu, S., Gao, Y., Zhang, X., Liu, G., Zhou, H., Lv, Y., Zhang, C., and Wang, Z.L. (2021). Breeze-wind-energy-powered autonomous wireless anemometer based on rolling contact-electrification. ACS Energy Lett. *6*, 2343–2350. https://doi.org/10.1021/acsenergylett.1c00704.

47. Zhang, L., Zhang, Y., Li, X., Feng, Y., Yu, B., Zhou, F., and Wang, D. (2022). Mechanism and regulation of peeling-electrification in adhesive interface. Nano Energy *95*, 107011. https://doi.org/10.1016/j.nanoen.2022.107011.

48. Chen, Y., Zhang, Y., Zhan, T., Lin, Z., Zhang, S.L., Zou, H., Zhang, G., Zou, C., and Wang, Z.L. (2019). An elastic triboelectric nanogenerator for harvesting random mechanical energy with multiple working modes. Adv. Mater. Technol. *4*, 1900075. https://doi.org/10.1002/admt.201900075.

49. Xu, L., Wu, H., Yao, G., Chen, L., Yang, X., Chen, B., Huang, X., Zhong, W., Chen, X., Yin, Z., and Wang, Z.L. (2018). Giant voltage enhancement via triboelectric charge supplement channel for self-powered electroadhesion. ACS Nano *12*, 10262–10271. https://doi.org/10.1021/acsnano.8b05359.

50. Liu, Y., Wen, J., Chen, B., Zheng, M., Liu, D., Liu, Y., Tang, W., Liu, J., Nan, D., and Wang, Z.L. (2020). Electro-blown spinning driven by cylindrical rotating triboelectric nanogenerator and its applications for fabricating nanofibers. Appl. Mater. Today *19*, 100631. https://doi.org/10.1016/j.apmt.2020.100631.

51. Liu, S., Li, Y., Guo, W., Huang, X., Xu, L., Lai, Y.-C., Zhang, C., and Wu, H. (2019). Triboelectric nanogenerators enabled sensing and actuation for robotics. Nano

Cell Reports
Physical Science
Review

CellPress
OPEN ACCESS

Energy *65*, 104005. https://doi.org/10.1016/j.nanoen.2019.104005.

52. Lahariya, M., Innes, C., Develder, C., and Ramamoorthy, S. (2022). Learning physics-informed simulation models for soft robotic manipulation: a case study with dielectric elastomer actuators. Preprint at arXiv.

53. Ren, Z., Kim, S., Ji, X., Zhu, W., Niroui, F., Kong, J., and Chen, Y. (2022). A high-lift micro-aerial-robot powered by low-voltage and long-endurance dielectric elastomer actuators. Adv. Mater. *34*, 2106757. https://doi.org/10.1002/adma.202106757.

54. Chen, X., Jiang, T., Yao, Y., Xu, L., Zhao, Z., and Wang, Z.L. (2016). Stimulating acrylic elastomers by a triboelectric nanogenerator – toward self-powered electronic skin and artificial muscle. Adv. Funct. Mater. *26*, 4906–4913. https://doi.org/10.1002/adfm.201600624.

55. Qu, X., Ma, X., Shi, B., Li, H., Zheng, L., Wang, C., Liu, Z., Fan, Y., Chen, X., Li, Z., and Wang, Z.L. (2021). Refreshable Braille display system based on triboelectric nanogenerator and dielectric elastomer. Adv. Funct. Mater. *31*, 2006612. https://doi.org/10.1002/adfm.202006612.

56. Liu, N., Martinez, T., Walter, A., Civet, Y., and Perriard, Y. (2022). Control-oriented modeling and analysis of tubular dielectric elastomer actuators dedicated to cardiac assist devices. IEEE Robot. Autom. Lett. *7*, 4361–4367. https://doi.org/10.1109/lra.2022.3148981.

57. Li, C., Yin, Y., Wang, B., Zhou, T., Wang, J., Luo, J., Tang, W., Cao, R., Yuan, Z., Li, N., et al. (2017). Self-powered electrospinning system driven by a triboelectric nanogenerator. ACS Nano *11*, 10439–10445. https://doi.org/10.1021/acsnano.7b05626.

58. Yang, D., Feng, Y., Wang, B., Liu, Y., Zheng, Y., Sun, X., Peng, J., Feng, M., and Wang, D. (2021). An asymmetric AC electric field of triboelectric nanogenerator for efficient water/oil emulsion separation. Nano Energy *90*, 106641. https://doi.org/10.1016/j.nanoen.2021.106641.

59. Chen, X., Wu, Y., Yu, A., Xu, L., Zheng, L., Liu, Y., Li, H., and Lin Wang, Z. (2017). Self-powered modulation of elastomeric optical grating by using triboelectric nanogenerator. Nano Energy *38*, 91–100. https://doi.org/10.1016/j.nanoen.2017.05.039.

60. Cheng, G., Zheng, H., Yang, F., Zhao, L., Zheng, M., Yang, J., Qin, H., Du, Z., and Wang, Z.L. (2018). Managing and maximizing the output power of a triboelectric nanogenerator by controlled tip–electrode air-discharging and application for UV sensing. Nano Energy *44*, 208–216. https://doi.org/10.1016/j.nanoen.2017.11.062.

61. Yu, J., Wei, X., Guo, Y., Zhang, Z., Rui, P., Zhao, Y., Zhang, W., Shi, S., and Wang, P. (2021). Self-powered droplet manipulation system for microfluidics based on triboelectric nanogenerator harvesting rotary energy. Lab Chip *21*, 284–295. https://doi.org/10.1039/d0lc00994f.

62. Wang, H., Wu, Y., and Wang, J. (2022). Triboelectric charging of melt-blown nonwoven filters with high filtration efficiency.

Sci. Rep. *12*, 1146. https://doi.org/10.1038/s41598-022-04838-3.

63. Guo, X., Bian, J., Bai, Y., Ma, Z., Yang, S., and Wang, Z. (2022). Trap-independent mechanoluminescence in ZnB2O4:Mn2+/PDMS composite elastomer with self-recovery activity. Chem. Phys. Lett. *787*, 139235. https://doi.org/10.1016/j.cplett.2021.139235.

64. Feng, A., and Smet, P.F. (2018). A review of mechanoluminescence in inorganic solids: compounds, mechanisms, models and applications. Materials *11*, 484. https://doi.org/10.3390/ma11040484.

65. Wang, W., Wang, Z., Zhang, J., Zhou, J., Dong, W., and Wang, Y. (2022). Contact electrification induced mechanoluminescence. Nano Energy *94*, 106920. https://doi.org/10.1016/j.nanoen.2022.106920.

66. Lin, Q., Li, Z., and Yuan, Q. (2019). Recent advances in autofluorescence-free biosensing and bioimaging based on persistent luminescence nanoparticles. Chin. Chem. Lett. *30*, 1547–1556. https://doi.org/10.1016/j.cclet.2019.06.016.

67. Liang, L., Chen, N., Jia, Y., Ma, Q., Wang, J., Yuan, Q., and Tan, W. (2019). Recent progress in engineering near-infrared persistent luminescence nanoprobes for time-resolved biosensing/bioimaging. Nano Res. *12*, 1279–1292. https://doi.org/10.1007/s12274-019-2343-6.

68. Zhang, J.-C., Wang, X., Marriott, G., and Xu, C.-N. (2019). Trap-controlled mechanoluminescent materials. Prog. Mater. Sci. *103*, 678–742. https://doi.org/10.1016/j.pmatsci.2019.02.001.

69. Zhang, H., Peng, D., Wang, W., Dong, L., and Pan, C. (2015). Mechanically induced light emission and infrared-laser-induced upconversion in the Er-doped CaZnOS multifunctional piezoelectric semiconductor for optical pressure and temperature sensing. J. Phys. Chem. C *119*, 28136–28142. https://doi.org/10.1021/acs.jpcc.5b10302.

70. Su, L., Wang, H., and Zi, Y. (2021). Recent progress of triboelectrification-induced electroluminescence: from fundaments to applications. J. Phys. Mater. *4*, 042001. https://doi.org/10.1088/2515-7639/abfcab.

71. Li, H., Zhang, Y., Dai, H., Tong, W., Zhou, Y., Zhao, J., and An, Q. (2018). A self-powered porous ZnS/PVDF-HFP mechanoluminescent composite film that converts human movement into eye-readable light. Nanoscale *10*, 5489–5495. https://doi.org/10.1039/c8nr00379c.

72. Collins, A.L., Camara, C.G., Van Cleve, E., and Putterman, S.J. (2018). Simultaneous measurement of triboelectrification and triboluminescence of crystalline materials. Rev. Sci. Instrum. *89*, 013901. https://doi.org/10.1063/1.5006811.

73. Obreimoff, J.W., and Kapitza, P.L. (1930). The splitting strength of mica. Proc. R. Soc. London Ser. A-Math. Phys. Eng. Sci. *127*, 290–297.

74. Camara, C.G., Escobar, J.V., Hird, J.R., and Putterman, S.J. (2008). Correlation between nanosecond X-ray flashes and stick–slip

friction in peeling tape. Nature *455*, 1089–1092. https://doi.org/10.1038/nature07378.

75. Xie, Y., and Li, Z. (2018). Triboluminescence: recalling interest and new aspects. Inside Chem. *4*, 943–971. https://doi.org/10.1016/j.chempr.2018.01.001.

76. Hu, J., and Song, Y. (2022). Piezoelectric modulus prediction using machine learning and graph neural networks. Chem. Phys. Lett. *791*, 139359. https://doi.org/10.1016/j.cplett.2022.139359.

77. Wang, Z.L., and Song, J. (2006). Piezoelectric nanogenerators based on zinc oxide nanowire arrays. Science *312*, 242–246. https://doi.org/10.1126/science.1124005.

78. Dagdeviren, C., Su, Y., Joe, P., Yona, R., Liu, Y., Kim, Y.-S., Huang, Y., Damadoran, A.R., Xia, J., Martin, L.W., et al. (2014). Conformable amplified lead zirconate titanate sensors with enhanced piezoelectric response for cutaneous pressure monitoring. Nat. Commun. *5*, 4496. https://doi.org/10.1038/ncomms5496.

79. Fan, F.-R., Tian, Z.-Q., and Lin Wang, Z. (2012). Flexible triboelectric generator. Nano Energy *1*, 328–334. https://doi.org/10.1016/j.nanoen.2012.01.004.

80. Jie, Y., Jia, X., Zou, J., Chen, Y., Wang, N., Wang, Z.L., and Cao, X. (2018). Natural leaf made triboelectric nanogenerator for harvesting environmental mechanical energy. Adv. Energy Mater. *8*, 1703133. https://doi.org/10.1002/aenm.201703133.

81. Seung, W., Yoon, H.-J., Kim, T.Y., Ryu, H., Kim, J., Lee, J.-H., Lee, J.H., Kim, S., Park, Y.K., Park, Y.J., and Kim, S.-W. (2017). Nanogenerators: boosting power-generating performance of triboelectric nanogenerators via artificial control of ferroelectric polarization and dielectric properties (adv. Energy mater. 2/2017). Adv. Energy Mater. *7*, 1600988. https://doi.org/10.1002/aenm.201770007.

82. Wang, X., Yang, B., Liu, J., Zhu, Y., Yang, C., and He, Q. (2016). A flexible triboelectric-piezoelectric hybrid nanogenerator based on P(VDF-TrFE) nanofibers and PDMS/MWCNT for wearable devices. Sci. Rep. *6*, 36409. https://doi.org/10.1038/srep36409.

83. Tang, Y.-Y., Li, P.-F., Liao, W.-Q., Shi, P.-P., You, Y.-M., and Xiong, R.-G. (2018). Multiaxial molecular ferroelectric thin films bring light to practical applications. J. Am. Chem. Soc. *140*, 8051–8059. https://doi.org/10.1021/jacs.8b04600.

84. Kalyani, A.K., Garg, R., and Ranjan, R. (2009). Competing A-site and B-site driven ferro-electric instabilities in the (1−x)PbTiO3-(x)BiAlO3 system. Appl. Phys. Lett. *94*, 202903. https://doi.org/10.1063/1.3136855.

85. Ye, H.-Y., Tang, Y.-Y., Li, P.-F., Liao, W.-Q., Gao, J.-X., Hua, X.-N., Cai, H., Shi, P.-P., You, Y.-M., and Xiong, R.-G. (2018). Metal-free three-dimensional perovskite ferroelectrics. Science *361*, 151–155. https://doi.org/10.1126/science.aas9330.

86. Zhang, R., Hummelgård, M., Örtegren, J., Song, M., Olsen, M., Andersson, H., Blomquist, N., and Olin, H. (2022). High performance single material-based

triboelectric nanogenerators made of hetero-triboelectric half-cell plant skins. Nano Energy *94*, 106959. https://doi.org/10.1016/j.nanoen.2022.106959.

87. Zhao, Z., Zhou, L., Li, S., Liu, D., Li, Y., Gao, Y., Liu, Y., Dai, Y., Wang, J., and Wang, Z.L. (2021). Selection rules of triboelectric materials for direct-current triboelectric nanogenerator. Nat. Commun. *12*, 4686. https://doi.org/10.1038/s41467-021-25046-z.

88. Yang, Y., Zhang, H., Chen, J., Jing, Q., Zhou, Y.S., Wen, X., and Wang, Z.L. (2013). Single-electrode-based sliding triboelectric nanogenerator for self-powered displacement vector sensor system. ACS Nano *7*, 7342–7351. https://doi.org/10.1021/nn403021m.

89. Su, L., Zhao, Z.X., Li, H.Y., Yuan, J., Wang, Z.L., Cao, G.Z., and Zhu, G. (2015). High-performance organolead halide perovskite-based self-powered triboelectric photodetector. ACS Nano *9*, 11310–11316. https://doi.org/10.1021/acsnano.5b04995.

90. Zou, H., Guo, L., Xue, H., Zhang, Y., Shen, X., Liu, X., Wang, P., He, X., Dai, G., Jiang, P., et al. (2020). Quantifying and understanding the triboelectric series of inorganic non-metallic materials. Nat. Commun. *11*, 2093. https://doi.org/10.1038/s41467-020-15926-1.

91. Zhang, R., and Olin, H. (2020). Material choices for triboelectric nanogenerators: a critical review. EcoMat *2*, e12062. https://doi.org/10.1002/eom2.12062.

92. Yao, C., Yin, X., Yu, Y., Cai, Z., and Wang, X. (2017). Chemically functionalized natural cellulose materials for effective triboelectric nanogenerator development. Adv. Funct. Mater. *27*, 1700794. https://doi.org/10.1002/adfm.201700794.

93. Chen, J., Guo, H., He, X., Liu, G., Xi, Y., Shi, H., and Hu, C. (2016). Enhancing performance of triboelectric nanogenerator by filling high dielectric nanoparticles into sponge PDMS film. ACS Appl. Mater. Interfaces *8*, 736–744. https://doi.org/10.1021/acsami.5b09907.

94. Pratap, A., Gogurla, N., and Kim, S. (2022). Elastic and skin-contact triboelectric nanogenerators and their applicability in energy harvesting and tactile sensing. ACS Appl. Electron. Mater. *4*, 1124–1131. https://doi.org/10.1021/acsaelm.1c01246.

95. Zu, G., Wei, Y., Sun, C., and Yang, X. (2022). Humidity-resistant, durable, wearable single-electrode triboelectric nanogenerator for mechanical energy harvesting. J. Mater. Sci. *57*, 2813–2824. https://doi.org/10.1007/s10853-021-06696-2.

96. Yang, Y., Zhang, H., Lin, Z.-H., Zhou, Y.S., Jing, Q., Su, Y., Yang, J., Chen, J., Hu, C., and Wang, Z.L. (2013). Human skin based triboelectric nanogenerators for harvesting biomechanical energy and as self-powered active tactile sensor system. ACS Nano *7*, 9213–9222. https://doi.org/10.1021/nn403838y.

97. Slabov, V., Kopyl, S., Soares dos Santos, M.P., and Kholkin, A.L. (2020). Natural and eco-friendly materials for triboelectric energy harvesting. Micro Nano Lett. *12*, 42. https://doi.org/10.1007/s40820-020-0373-y.

98. Guo, Y., Zhang, X.-S., Wang, Y., Gong, W., Zhang, Q., Wang, H., and Brugger, J. (2018). All-fiber hybrid piezoelectric-enhanced triboelectric nanogenerator for wearable gesture monitoring. Nano Energy *48*, 152–160. https://doi.org/10.1016/j.nanoen.2018.03.033.

99. Han, M., Chen, X., Yu, B., and Zhang, H. (2015). Coupling of piezoelectric and triboelectric effects: from theoretical analysis to experimental verification. Adv. Electron. Mater. *1*, 1500187. https://doi.org/10.1002/aelm.201500187.

100. Xu, Q., Wen, J., and Qin, Y. (2021). Development and outlook of high output piezoelectric nanogenerators. Nano Energy *86*, 106080. https://doi.org/10.1016/j.nanoen.2021.106080.

101. Kim, M.P., Um, D.-S., Shin, Y.-E., and Ko, H. (2021). High-performance triboelectric devices via dielectric polarization: a review. Nanoscale Res. Lett. *16*, 35. https://doi.org/10.1186/s11671-021-03492-4.

102. Synhaivskyi, O., Albertini, D., Gaffuri, P., Chauveau, J.-M., Consonni, V., Gautier, B., and Bremond, G. (2021). Evidence of piezoelectric potential and screening effect in single highly doped ZnO:Ga and ZnO:Al nanowires by advanced scanning probe microscopy. J. Phys. Chem. C *125*, 15373–15383. https://doi.org/10.1021/acs.jpcc.1c00926.

103. Smeltere, I., Antonova, M., Kalvane, A., Grigs, O., and Livinsh, M.J.M.S. (1970). The effect of dopants on sintering and microstructure of lead-free KNN ceramics. Mater. Sci. *17*, 62–64. https://doi.org/10.5755/j01.ms.17.1.251.

104. Småbråten, D.R., Holstad, T.S., Evans, D.M., Yan, Z., Bourret, E., Meier, D., and Selbach, S.M. (2020). Domain wall mobility and roughening in doped ferroelectric hexagonal manganites. Phys. Rev. Res. *2*, 033159. https://doi.org/10.1103/physrevresearch.2.033159.

105. Shimojo, Y., Wang, R., Sekiya, T., Nakamura, T., and Cross, L.E. (2003). MPB phase diagram and ferroelectric properties in the PbTiO$_3$-BiScO$_3$ system. Ferroelectrics *284*, 121–128. https://doi.org/10.1080/00150190390204763.

106. Shankar, U., Kumar, N., Narayan, B., Swain, D., Senyshyn, A., and Ranjan, R. (2019). Large electromechanical response in ferroelectrics: beyond the morphotropic phase boundary paradigm. Phys. Rev. B *100*, 094101. https://doi.org/10.1103/physrevb.100.094101.

107. Wang, Y., Yang, X., Yu, X., Duan, J., Yang, Q., Duan, Y., and Tang, Q. (2020). Triboelectric charging behaviors and photoinduced enhancement of alkaline earth ions doped inorganic perovskite triboelectric nanogenerators. Nano Energy *77*, 105280. https://doi.org/10.1016/j.nanoen.2020.105280.

108. Fan, F.-R., Lin, L., Zhu, G., Wu, W., Zhang, R., and Wang, Z.L. (2012). Transparent triboelectric nanogenerators and self-powered pressure sensors based on micropatterned plastic films. Nano Lett. *12*, 3109–3114. https://doi.org/10.1021/nl300988z.

109. Wu, C., Kim, T.W., Park, J.H., An, H., Shao, J., Chen, X., and Wang, Z.L. (2017). Enhanced triboelectric nanogenerators based on MoS$_2$ monolayer nanocomposites acting as electron-acceptor layers. ACS Nano *11*, 8356–8363. https://doi.org/10.1021/acsnano.7b03657.

110. Zhao, Q.-L., He, G.-P., Di, J.-J., Song, W.-L., Hou, Z.-L., Tan, P.-P., Wang, D.-W., and Cao, M.-S. (2017). Flexible semitransparent energy harvester with high pressure sensitivity and power density based on laterally aligned PZT single-crystal nanowires. ACS Appl. Mater. Interfaces *9*, 24696–24703. https://doi.org/10.1021/acsami.7b03929.

111. Tsujioka, T., and Tsuji, K. (2012). Metal-vapor deposition modulation on soft polymer surfaces. Appl. Phys. Express *5*, 021601. https://doi.org/10.1143/apex.5.021601.

112. Ahmad, Z., Prasad, A., and Prasad, K. (2009). A comparative approach to predicting effective dielectric, piezoelectric and elastic properties of PZT/PVDF composites. Physica B Condens. Matter *404*, 3637–3644. https://doi.org/10.1016/j.physb.2009.06.009.

113. Chandran, A.M., and Mural, P.K.S. (2022). Surface silanized MWCNTs doped PVDF nanocomposite with self-organized dipoles: an intrinsic study on the dielectric, piezoelectric, ferroelectric, and energy harvesting phenomenology. Sustain. Energy Fuels *6*, 1641–1653. https://doi.org/10.1039/d1se01256h.

114. Shoorangiz, M., Sherafat, Z., and Bagherzadeh, E. (2022). CNT loaded PVDF-KNN nanocomposite films with enhanced piezoelectric properties. Ceram. Int. *48*, 15180–15188. https://doi.org/10.1016/j.ceramint.2022.02.047.

115. Zargari, S., Rezania, A., Koozehkanani, Z.D., Veladi, H., Sobhi, J., and Rosendahl, L. (2022). Effect of the inherent capacitance optimization on the output performance of triboelectric nanogenerators. Nano Energy *92*, 106740. https://doi.org/10.1016/j.nanoen.2021.106740.

116. Ko, Y.H., Lee, S.H., Leem, J.W., and Yu, J.S. (2014). High transparency and triboelectric charge generation properties of nano-patterned PDMS. RSC Adv. *4*, 10216. https://doi.org/10.1039/c3ra47199c.

117. Jeong, C.K., Baek, K.M., Niu, S., Nam, T.W., Hur, Y.H., Park, D.Y., Hwang, G.-T., Byun, M., Wang, Z.L., Jung, Y.S., and Lee, K.J. (2014). Topographically-designed triboelectric nanogenerator via block copolymer self-assembly. Nano Lett. *14*, 7031–7038. https://doi.org/10.1021/nl503402c.

118. Feng, Y., Zheng, Y., Ma, S., Wang, D., Zhou, F., and Liu, W. (2016). High output polypropylene nanowire array triboelectric nanogenerator through surface structural control and chemical modification. Nano Energy *19*, 48–57. https://doi.org/10.1016/j.nanoen.2015.11.017.

119. Huang, T., Lu, M., Yu, H., Zhang, Q., Wang, H., and Zhu, M. (2015). Enhanced power output of a triboelectric nanogenerator composed of electrospun nanofiber mats doped with graphene oxide. Sci. Rep. *5*, 13942. https://doi.org/10.1038/srep13942.

120. Yang, Y., Yang, W., Wang, Y., Zeng, X., and Hu, Y. (2022). A mechanically induced artificial

Cell Reports
Physical Science
Review

CellPress
OPEN ACCESS

potential barrier and its tuning mechanism on performance of piezoelectric PN junctions. Nano Energy 92, 106741. https://doi.org/10.1016/j.nanoen.2021.106741.

121. Chai, B., Shi, K., Zou, H., Jiang, P., Wu, Z., and Huang, X. (2022). Conductive interlayer modulated ferroelectric nanocomposites for high performance triboelectric nanogenerator. Nano Energy 91, 106668. https://doi.org/10.1016/j.nanoen.2021.106668.

122. Xu, L., Bu, T.Z., Yang, X.D., Zhang, C., and Wang, Z.L. (2018). Ultrahigh charge density realized by charge pumping at ambient conditions for triboelectric nanogenerators. Nano Energy 49, 625–633. https://doi.org/10.1016/j.nanoen.2018.05.011.

123. Liu, W., Wang, Z., Wang, G., Liu, G., Chen, J., Pu, X., Xi, Y., Wang, X., Guo, H., Hu, C., and Wang, Z.L. (2019). Integrated charge excitation triboelectric nanogenerator. Nat. Commun. 10, 1426. https://doi.org/10.1038/s41467-019-09464-8.

124. Xie, Y., Wang, S., Lin, L., Jing, Q., Lin, Z.-H., Niu, S., Wu, Z., and Wang, Z.L. (2013). Rotary triboelectric nanogenerator based on a hybridized mechanism for harvesting wind energy. ACS Nano 7, 7119–7125. https://doi.org/10.1021/nn402477h.

125. Zhou, M., Al-Furjan, M.S.H., Zou, J., and Liu, W. (2018). A review on heat and mechanical energy harvesting from human – principles, prototypes and perspectives. Renew. Sust. Energ. Rev. 82, 3582–3609. https://doi.org/10.1016/j.rser.2017.10.102.

126. Xu, L., Zhang, Z., Gao, F., Zhao, X., Xun, X., Kang, Z., Liao, Q., and Zhang, Y. (2021). Self-powered ultrasensitive pulse sensors for noninvasive multi-indicators cardiovascular monitoring. Nano Energy 81, 105614. https://doi.org/10.1016/j.nanoen.2020.105614.

127. Peng, X., Dong, K., Ning, C., Cheng, R., Yi, J., Zhang, Y., Sheng, F., Wu, Z., and Wang, Z.L. (2021). All-nanofiber self-powered skin-interfaced real-time respiratory monitoring system for obstructive sleep apnea-hypopnea syndrome diagnosing. Adv. Funct. Mater. 31, 2103559. https://doi.org/10.1002/adfm.202103559.

128. Ouyang, H., Liu, Z., Li, N., Shi, B., Zou, Y., Xie, F., Ma, Y., Li, Z., Li, H., Zheng, Q., et al. (2019). Symbiotic cardiac pacemaker. Nat. Commun. 10, 1821. https://doi.org/10.1038/s41467-019-09851-1.

129. Jeong, S.-H., Lee, Y., Lee, M.-G., Song, W.J., Park, J.-U., and Sun, J.-Y. (2021). Accelerated wound healing with an ionic patch assisted by a triboelectric nanogenerator. Nano Energy 79, 105463. https://doi.org/10.1016/j.nanoen.2020.105463.

130. Wang, C., Qu, X., Zheng, Q., Liu, Y., Tan, P., Shi, B., Ouyang, H., Chao, S., Zou, Y., Zhao, C., et al. (2021). Stretchable, self-healing, and skin-mounted active sensor for multipoint muscle function assessment. ACS Nano 15, 10130–10140. https://doi.org/10.1021/acsnano.1c02010.

131. Dagdeviren, C., Shi, Y., Joe, P., Ghaffari, R., Balooch, G., Usgaonkar, K., Gur, O., Tran, P.L., Crosby, J.R., Meyer, M., et al. (2015).

Conformal piezoelectric systems for clinical and experimental characterization of soft tissue biomechanics. Nat. Mater. 14, 728–736. https://doi.org/10.1038/nmat4289.

132. Pascual-Valdunciel, A., Rajagopal, A., Pons, J.L., and Delp, S. (2022). Non-invasive electrical stimulation of peripheral nerves for the management of tremor. J. Neurol. Sci. 435, 120195. https://doi.org/10.1016/j.jns.2022.120195.

133. Hwang, G.-T., Kim, Y., Lee, J.-H., Oh, S., Jeong, C.K., Park, D.Y., Ryu, J., Kwon, H., Lee, S.-G., Joung, B., et al. (2015). Self-powered deep brain stimulation via a flexible PIMNT energy harvester. Energy Environ. Sci. 8, 2677–2684. https://doi.org/10.1039/c5ee01593f.

134. Blanquer, A., Careta, O., Anido-Varela, L., Aranda, A., Ibáñez, E., Esteve, J., Nogués, C., and Murillo, G. (2022). Biocompatibility and electrical stimulation of skeletal and smooth muscle cells cultured on piezoelectric nanogenerators. Int. J. Mol. Sci. 23, 432. https://doi.org/10.3390/ijms23010432.

135. Li, G., Zhu, Q., Wang, B., Luo, R., Xiao, X., Zhang, Y., Ma, L., Feng, X., Huang, J., Sun, X., et al. (2021). Rejuvenation of senescent bone marrow mesenchymal stromal cells by pulsed triboelectric stimulation. Sci. Adv. 8, 2100964. https://doi.org/10.1002/advs.202100964.

136. Zhou, M., Huang, M., Zhong, H., Xing, C., An, Y., Zhu, R., Jia, Z., Qu, H., Zhu, S., Liu, S., et al. (2022). Contact separation triboelectric nanogenerator based neural interfacing for effective sciatic nerve restoration. Adv. Funct. Mater. 32, 2200269.

137. Kao, F.-C., Ho, H.-H., Chiu, P.-Y., Hsieh, M.-K., Liao, J.C., Lai, P.-L., Huang, Y.-F., Dong, M.-Y., Tsai, T.-T., and Lin, Z.-H. (2022). Self-assisted wound healing using piezoelectric and triboelectric nanogenerators. Sci. Technol. Adv. Mater. 23, 1–16. https://doi.org/10.1080/14686996.2021.2015249.

138. Ouyang, Q., Feng, X., Kuang, S., Panwar, N., Song, P., Yang, C., Yang, G., Hemu, X., Zhang, G., Yoon, H.S., et al. (2019). Self-powered, on-demand transdermal drug delivery system driven by triboelectric nanogenerator. Nano Energy 62, 610–619. https://doi.org/10.1016/j.nanoen.2019.05.056.

139. Liang, L., Tang, Y., Hu, X., Wang, J., Xiao, S., Li, D., Fu, L., Li, Z., and Yuan, Q. (2019). Photoresponsive biomimetic protocells for near-infrared-light-regulated phototheranostics. CCS Chem 1, 490–501. https://doi.org/10.31635/ccschem.019.20180033.

140. Yu, X., Wang, S., Zhang, X., Qi, A., Qiao, X., Liu, Z., Wu, M., Li, L., and Wang, Z.L. (2018). Heterostructured nanorod array with piezophototronic and plasmonic effect for photodynamic bacteria killing and wound healing. Nano Energy 46, 29–38. https://doi.org/10.1016/j.nanoen.2018.01.033.

141. Shlomy, I., Divald, S., Tadmor, K., Leichtmann-Bardoogo, Y., Arami, A., and Maoz, B.M. (2021). Restoring tactile sensation using a triboelectric nanogenerator. ACS Nano 15, 11087–11098. https://doi.org/10.1021/acsnano.0c10141.

142. Chun, S., Kim, J.-S., Yoo, Y., Choi, Y., Jung, S.J., Jang, D., Lee, G., Song, K.-I., Nam, K.S., Youn, I., et al. (2021). An artificial neural tactile sensing system. Nat. Electron. 4, 429–438. https://doi.org/10.1038/s41928-021-00585-x.

143. Liu, Y., Zhu, Y., Liu, J., Zhang, Y., Liu, J., and Zhai, J. (2018). Design of bionic cochlear basilar membrane acoustic sensor for frequency selectivity based on film triboelectric nanogenerator. Nanoscale Res. Lett. 13, 191. https://doi.org/10.1186/s11671-018-2593-3.

144. Wang, X., Song, W.-Z., You, M.-H., Zhang, J., Yu, M., Fan, Z., Ramakrishna, S., and Long, Y.-Z. (2018). Bionic single-electrode electronic skin unit based on piezoelectric nanogenerator. ACS Nano 12, 8588–8596. https://doi.org/10.1021/acsnano.8b04244.

145. Lai, Y.-C., Deng, J., Liu, R., Hsiao, Y.-C., Zhang, S.L., Peng, W., Wu, H.-M., Wang, X., and Wang, Z.L. (2018). Actively perceiving and responsive soft robots enabled by self-powered, highly extensible, and highly sensitive triboelectric proximity- and pressure-sensing skins. Adv. Mater. 30, 1801114. https://doi.org/10.1002/adma.201801114.

146. Gao, Z., Ren, B., Fang, Z., Kang, H., Han, J., and Li, J. (2021). Accurate recognition of object contour based on flexible piezoelectric and piezoresistive dual mode strain sensors. Sens. Actuator A Phys. 332, 113121. https://doi.org/10.1016/j.sna.2021.113121.

147. Jin, T., Sun, Z., Li, L., Zhang, Q., Zhu, M., Zhang, Z., Yuan, G., Chen, T., Tian, Y., Hou, X., and Lee, C. (2020). Triboelectric nanogenerator sensors for soft robotics aiming at digital twin applications. Nat. Commun. 11, 5381. https://doi.org/10.1038/s41467-020-19059-3.

148. Chen, J., Zhu, G., Yang, J., Jing, Q., Bai, P., Yang, W., Qi, X., Su, Y., and Wang, Z.L. (2015). Personalized keystroke dynamics for self-powered human–machine interfacing. ACS Nano 9, 105–116. https://doi.org/10.1021/nn506832w.

149. Cao, Y., Yang, Y., Qu, X., Shi, B., Xu, L., Xue, J., Wang, C., Bai, Y., Gai, Y., Luo, D., and Li, Z. (2022). A self-powered triboelectric hybrid coder for human–machine interaction. Small Methods 6, 2101529. https://doi.org/10.1002/smtd.202101529.

150. Dhakar, L., Pitchappa, P., Tay, F.E.H., and Lee, C. (2016). An intelligent skin based self-powered finger motion sensor integrated with triboelectric nanogenerator. Nano Energy 19, 532–540. https://doi.org/10.1016/j.nanoen.2015.04.020.

151. Lin, Z., Wu, Z., Zhang, B., Wang, Y.-C., Guo, H., Liu, G., Chen, C., Chen, Y., Yang, J., and Wang, Z.L. (2019). A triboelectric nanogenerator-based smart insole for multifunctional gait monitoring. Adv. Mater. Technol. 4, 1800360. https://doi.org/10.1002/admt.201800360.

152. Xi, Y., Hua, J., and Shi, Y. (2020). Noncontact triboelectric nanogenerator for human motion monitoring and energy harvesting. Nano Energy 69, 104390. https://doi.org/10.1016/j.nanoen.2019.104390.

CellPress
OPEN ACCESS

Cell Reports
Physical Science
Review

153. Nair, M.P., Teo, A.J.T., and Li, K.H.H. (2021). Acoustic biosensors and microfluidic devices in the decennium: principles and applications. Micromachines 13, 24. https://doi.org/10.3390/mi13010024.

154. Shen, Q., Xie, X., Peng, M., Sun, N., Shao, H., Zheng, H., Wen, Z., and Sun, X. (2018). Self-powered sensing: self-powered vehicle emission testing system based on coupling of triboelectric and chemoresistive effects (adv. Funct. Mater. 10/2018). Adv. Funct. Mater. 28, 1870067. https://doi.org/10.1002/adfm.201870067.

155. Wang, H., Wu, H., Hasan, D., He, T., Shi, Q., and Lee, C. (2017). Self-powered dual-mode amenity sensor based on the water–air triboelectric nanogenerator. ACS Nano 11, 10337–10346. https://doi.org/10.1021/acsnano.7b05213.

156. Zhang, H., Yang, Y., Su, Y., Chen, J., Hu, C., Wu, Z., Liu, Y., Ping Wong, C., Bando, Y., and Wang, Z.L. (2013). Triboelectric nanogenerator as self-powered active sensors for detecting liquid/gaseous water/ethanol. Nano Energy 2, 693–701. https://doi.org/10.1016/j.nanoen.2013.08.004.

157. Chen, B.D., Tang, W., He, C., Jiang, T., Xu, L., Zhu, L.P., Gu, G.Q., Chen, J., Shao, J.J., Luo, J.J., and Wang, Z.L. (2018). Ultrafine capillary-tube triboelectric nanogenerator as active sensor for microliquid biological and chemical sensing. Adv. Mater. Technol. 3, 1700229. https://doi.org/10.1002/admt.201700229.

158. Zhao, Z., Pu, X., Du, C., Li, L., Jiang, C., Hu, W., and Wang, Z.L. (2016). Freestanding flag-type triboelectric nanogenerator for harvesting high-altitude wind energy from arbitrary directions. ACS Nano 10, 1780–1787. https://doi.org/10.1021/acsnano.5b07157.

159. Xu, M., Zhao, T., Wang, C., Zhang, S.L., Li, Z., Pan, X., and Wang, Z.L. (2019). High power density tower-like triboelectric nanogenerator for harvesting arbitrary directional water wave energy. ACS Nano 13, 1932–1939. https://doi.org/10.1021/acsnano.8b08274.

160. Chen, S., Gao, C., Tang, W., Zhu, H., Han, Y., Jiang, Q., Li, T., Cao, X., and Wang, Z. (2015). Self-powered cleaning of air pollution by wind driven triboelectric nanogenerator. Nano Energy 14, 217–225. https://doi.org/10.1016/j.nanoen.2014.12.013.

161. Wang, Z., Shi, Y., Liu, F., Wang, H., Liu, X., Sun, R., Lu, Y., Ji, L., Wang, Z.L., and Cheng, J. (2020). Distributed mobile ultraviolet light sources driven by ambient mechanical stimuli. Nano Energy 74, 104910. https://doi.org/10.1016/j.nanoen.2020.104910.

162. Xie, Z., Zeng, Z., Wang, Y., Yang, W., Xu, Y., Lu, X., Cheng, T., Zhao, H., and Wang, Z.L. (2020). Novel sweep-type triboelectric nanogenerator utilizing single freewheel for random triggering motion energy harvesting and driver habits monitoring. Nano Energy 68, 104360. https://doi.org/10.1016/j.nanoen.2019.104360.

163. Shi, Q., Zhang, Z., He, T., Sun, Z., Wang, B., Feng, Y., Shan, X., Salam, B., and Lee, C. (2020). Deep learning enabled smart mats as a scalable floor monitoring system. Nat. Commun. 11, 4609. https://doi.org/10.1038/s41467-020-18471-z.

164. Timilsina, S., Bashnet, R., Kim, S.H., Lee, K.H., and Kim, J.S. (2017). A life-time reproducible mechano-luminescent paint for the visualization of crack propagation mechanisms in concrete structures. Int. J. Fract. 101, 75–79. https://doi.org/10.1016/j.ijfatigue.2017.03.011.

165. Lei, R., Shi, Y., Wang, X., Tao, X., Zhai, H., and Chen, X. (2021). Water purification system based on self-powered ozone production. Nano Energy 88, 106230. https://doi.org/10.1016/j.nanoen.2021.106230.

166. Zhang, B., Chen, J., Jin, L., Deng, W., Zhang, L., Zhang, H., Zhu, M., Yang, W., and Wang, Z.L. (2016). Rotating-disk-based hybridized electromagnetic–triboelectric nanogenerator for sustainably powering wireless traffic volume sensors. ACS Nano 10, 6241–6247. https://doi.org/10.1021/acsnano.6b02384.

167. Lin, L., Hu, Y., Xu, C., Zhang, Y., Zhang, R., Wen, X., and Lin Wang, Z. (2013). Transparent flexible nanogenerator as self-powered sensor for transportation monitoring. Nano Energy 2, 75–81. https://doi.org/10.1016/j.nanoen.2012.07.019.

168. Zhang, Z., Shi, Q., He, T., Guo, X., Dong, B., Lee, J., and Lee, C. (2021). Artificial intelligence of toilet (AI-Toilet) for an integrated health monitoring system (IHMS) using smart triboelectric pressure sensors and image sensor. Nano Energy 90, 106517. https://doi.org/10.1016/j.nanoen.2021.106517.

169. Sohn, K.-S., Seo, S.Y., Kwon, Y.N., and Park, H.D. (2004). Direct observation of crack tip stress field using the mechanoluminescence of $SrAl_2O_4$:(Eu, Dy, Nd). J. Am. Ceram. Soc. 85, 712–714. https://doi.org/10.1111/j.1151-2916.2002.tb00158.x.

170. Li, C., Xu, C.-N., Ono, D., Ueno, N., and Kawabata, Y. (2012). Fracture prediction in reinforced concrete using mechanoluminescent sensor. J. Jpn. Soc. Exp. Mech. 12, s205–s208.

171. Zhang, L., Wang, Z., Wang, L., Zhang, Z., Chen, X., and Meng, L. (2021). Machine learning-based real-time visible fatigue crack growth detection. Digit. Commun. Netw. 7, 551–558. https://doi.org/10.1016/j.dcan.2021.03.003.

172. Liao, W.-Q., Tang, Y.-Y., Li, P.-F., You, Y.-M., and Xiong, R.-G. (2017). Large piezoelectric effect in a lead-free molecular ferroelectric thin film. J. Am. Chem. Soc. 139, 18071–18077. https://doi.org/10.1021/jacs.7b10449.